Rapid #: -20399593

CROSS REF ID: **302590**

LENDER: **BUB :: Main Library**

BORROWER: **MTH :: Main Library**

TYPE:	Article CC:CCG
JOURNAL TITLE:	International journal of bifurcation and chaos in applied sciences and engineering
USER JOURNAL TITLE:	International Journal of Bifurcation and Chaos
ARTICLE TITLE:	Complexity in a Hybrid van der Pol System
ARTICLE AUTHOR:	Naudot, Vincent,
VOLUME:	31
ISSUE:	13
MONTH:	
YEAR:	2021
PAGES:	2150194-
ISSN:	0218-1274
OCLC #:	

Processed by RapidX: 3/10/2023 4:54:14 AM

International Journal of Bifurcation and Chaos, Vol. 31, No. 13 (2021) 2150194 (20 pages)

DOI: 10.1142/S0218127421501947

Complexity in a Hybrid van der Pol System

Vincent Naudot
Department of Mathematical Sciences,
Florida Atlantic University, 777 Glades Road,
Boca Raton, FL 33431, USA

Shane Kepley
Department of Mathematics,
Rutgers, The State University of New Jersey,
New Brunswick, NJ, USA

William D. Kalies
Department of Mathematical Sciences,
Florida Atlantic University, 777 Glades Road,
Boca Raton, FL 33431, USA

Received October 23, 2020; Revised April 20, 2021

In this work, we study, from a numerical point of view, the dynamics of a specific hybrid map which is that of the kicked van der Pol system. The dynamics of this system is generated by a two-stage procedure: the first stage is the time-τ map of the vector field associated with the van der Pol equation, and the second stage is a translation. We propose a numerical method for computing local (un)stable manifolds of a given fixed point, which leads to high order polynomial parameterization of the embedding. Such a representation of the dynamics on the manifold is obtained in terms of a simple conjugacy relation and by constructing two contracting operators. We illustrate our techniques by plotting (for specific values of the parameters) both stable and unstable manifolds displaying homoclinic intersection. Furthermore, our numerical study reveals the presence of a strange attractor included in the closure of the unstable manifold of the fixed point.

Keywords: Hybrid map; unstable manifold; strange attractor.

1. Introduction

Understanding the dynamics of a given map on a manifold is a challenging task. In the planar case, which is the context of this article, examples such as that of the Hénon map [Hénon, 1976] or "Hénon-like" maps have been studied in various works, see for instance [Benedicks & Carlson, 1991; Heagy, 1992; Mora & Viana, 1993; Martens *et al.*, 2006; Naudot, 1996, 2002; Rychlik, 1990; Tucker, 1999, 2002].

A standard strategy consists in searching for the locus of fixed points, or periodic points (of low period), and studying their stability. In the structurally stable context our search is for sinks, sources, and saddles. In the case of a saddle, our interest is to describe the associated invariant manifolds, i.e. the stable and the unstable manifolds. Analysis of these sets is of great help in understanding the dynamics since they describe the skeleton of (at least part of) the global dynamics. Furthermore, the complexity of the dynamics is guaranteed in case of a homoclinic orbit [Palis & de Melo, 1980; Palis & Takens, 1993]. As a consequence, the system is chaotic. More precisely, horseshoes are present

near the homoclinic orbit and in particular, one deduces the existence of infinitely many periodic points of saddle type. In this article, our interest is with a specific map called the kicked van der Pol system defined by

$$\begin{cases} \dot{x} = y - \alpha\left(\dfrac{x^3}{3} - x\right), \\ \dot{y} = -x + f(t), \end{cases} \tag{1}$$

where

$$f(t) = \beta \sum_{n=0}^{\infty} \delta(t - n\tau),$$

δ being the Dirac distribution at 0 while τ, α and β are parameters. This system is the same as that presented by van der Pol [van der Pol & van der Mark, 1927], except that the forcing term proposed in [van der Pol & van der Mark, 1927] is given by $f(t) = \beta \sin(\tau t)$. In the present version, the forcing only occurs at specific times and takes the form of instantaneous τ-periodic "kicks", see [Heagy, 1992; Lin & Young, 2010; Ippolito & Naudot, 2016; Ippolito *et al.*, 2016; Ryals & Young, 2012] for more examples of kicked dynamics. System (1) is introduced and studied in [Ryals & Young, 2012]. The idea from the authors behind the choice of such a forcing instead of a continuous map is that the action of the time-τ map can be easily decomposed into a couple of steps and (hopefully) one gets a better understanding of the dynamics from the topological point of view. It is shown that the time-τ map associated to Eq. (1) can be expressed as

$$\mathbf{\Phi} = \mathbf{L} \circ \mathcal{X}_\tau, \tag{2}$$

where $\mathcal{X}_\tau$ is the time-τ map associated with the homogeneous part of Eq. (1) (commonly called the standard van der Pol Equation), i.e.

$$\mathcal{X} : \begin{cases} \dot{x} = y - \alpha\left(\dfrac{x^3}{3} - x\right), \\ \dot{y} = -x \end{cases} \tag{3}$$

and $\mathbf{L}$ represents the contributions of the kicks which has the form $\mathbf{L}(x, y) = (x, y + \beta)$ (see [Ryals & Young, 2012] for details). Such a map is also called a *hybrid map* in [Lu *et al.*, 2016]. Thanks to a very subtle topological approach, the authors in [Ryals & Young, 2012] show the existence of horseshoes for τ sufficiently large and for a wide range of the other parameters (α, β). Roughly speaking, their approach consists in studying the dynamics of the kicked system in Eq. (1) in a tubular neighborhood of the limit cycle observed for the unperturbed system of Eq. (3). The parameter τ is assumed to be much larger than the period of the limit cycle and the essential part of the dynamics is described by the dynamics of a one-dimensional map. The authors show that for a suitable range of parameters, the system should exhibit horseshoes and strange attractors. Supported by numerics, it is shown that the system possesses nontrivial attractors with a positive Lyapunov exponent and with an SRB measure [Wang & Young, 2008]. The authors also claim that the size of those attractors are quite small and focus on a tiny region in the parameter space.

The present paper aims, mainly thanks to a numerical approach, to partially complete the study proposed in [Ryals & Young, 2012] for smaller values of τ. Our investigation concerns values of the parameters near

$$\alpha = 2, \quad \beta = 2.7 \quad \text{and} \quad \tau = 3.4.$$

Observe that in our case, unlike in [Ryals & Young, 2012], τ is much smaller than the period of the limit cycle of the unperturbed system in Eq. (3) which, for the above values of α and β, is approximately 7.56. Our study is driven from a different point of view.

As we previously mentioned, when considering diffeomorphims chaos and strange attractors are often bounded by the unstable manifolds of periodic points [Benedicks & Carlson, 1991; Guckenheimer & Holmes, 1983; Hénon, 1976; Hirsch *et al.*, 1977; Mora & Viana, 1993]. We claim that this latter property also holds for the hybrid map defined in Eq. (2). In the analytic case, when a map is explicitly defined (for instance, when considering the Hénon map), computing the expansion of the invariant manifolds (stable and unstable) is a classical task and is completely understood thanks to the so-called parameterization method [van den Berg *et al.*, 2011; Cabré *et al.*, 2003, 2005; Gonzalez & James, 2017; Haro & de la Llave, 2006; Lessard *et al.*, 2015]. This latter technique is quickly revisited in this article for the sake of completeness. However, when dealing with a hybrid map, which cannot be written explicitly, the usual algorithms for computing parameterizations are not directly applicable, see [Lu *et al.*, 2016] for more discussion. To overcome this difficulty, an algorithm

is presented in [Lu *et al.*, 2016] to compute the invariant (stable and unstable) manifolds of a hyperbolic fixed point. The algorithm consists of iterating a contracting operator where the local unstable manifold is the corresponding fixed point. To implement this technique numerically, each output of the operator is interpolated using Lagrange polynomials. However, in [Lu *et al.*, 2016] the interpolation part of the algorithm has not been taken rigorously into consideration. In the present article, we complete the theory by constructing two operators: in Sec. 2.2, a first contracting operator (similar to the one developed in [Lu *et al.*, 2016]), and in Sec. 2.4, an interpolated version of the former operator (called *the reduced operator*), and we show that this latter operator is also a contraction near the fixed point.

After performing the algorithm for the system under consideration, we display these invariant manifolds together with a transverse homoclinic intersection. Furthermore, we construct a transitive (rather large) invariant set by plotting the orbit of a point chosen near the fixed point. Our numerics suggest that this invariant set possesses a positive Lyapunov exponent [Mora & Viana, 1993; Ryals & Young, 2012] and therefore we conjecture that this set is a strange attractor. Moreover, the superimposition of this attractor and the unstable manifold also suggests that the former is included in the closure of the latter.

The paper is organized as follows. In Sec. 2, we present the method to compute the local unstable manifold of a hyperbolic fixed point of hybrid map. We first briefly recall the parameterization method for computing invariant manifolds of analytic maps. We focus our presentation on the search for an unstable manifold as the stable manifold is just the unstable manifold associated with the inverse map. Roughly speaking, the parameterization method consists of recursively computing the coefficients of the local unstable manifold as a Taylor expansion. However, when we do not know the map explicitly, as in the case of a hybrid map, we cannot obtain a recursive formula for the coefficients. Therefore, we must modify the approach accordingly. We define two contracting operators in a space of planar curves, the latter is an interpolant for the former. The ensuing local unstable manifold being a fixed point of the first operator, is approximated by looking at the iterates of the second operator on the line tangent to the unstable direction.

In Sec. 3, we compute the variational equation to estimate the hybrid map at a given point as well as its first derivative with respect to the phase variables. We then deduce, thanks to Newton's method, the locus of a hyperbolic fixed point and the eigenvalues (together with their respective eigenspaces) of the linearization of the map at the fixed point. When $\alpha = 2$, $\beta = 2.7$ and $\tau = 3.4$, we apply the techniques developed in Sec. 2 and we display the plot of both manifolds (global unstable and local stable), emphasizing a transverse homoclinic intersection. We superimpose our result with the plot of a nontrivial attractor obtained by plotting (the tails of) the iterates under the hybrid map of a point (randomly chosen) near the fixed point. Finally, we conjecture that the resulting attractor is included in the closure of the unstable manifold.

2. Settings and Operators

Let $\mathbf{p} = (p_1, p_2)$ be a hyperbolic fixed point of an analytic map

$$\mathbf{\Phi} : \mathcal{D} \to \mathbb{R}^2, \quad (x, y) \mapsto (\Phi_1(x, y), \Phi_2(x, y)),$$

where $\mathcal{D} \subset \mathbb{R}^2$ is an open set. Assume that λ and μ are the eigenvalues of $d\mathbf{\Phi}(\mathbf{p})$ and satisfy $0 < |\lambda| < 1 < |\mu|$. We choose

$$\mathbf{U}_+ = \begin{pmatrix} \mathrm{U}_{+,1} \\ \mathrm{U}_{+,2} \end{pmatrix}, \quad \left(\text{respectively } \mathbf{U}_- = \begin{pmatrix} \mathrm{U}_{-,1} \\ \mathrm{U}_{-,2} \end{pmatrix} \right) \tag{4}$$

an eigenvector of $d\mathbf{\Phi}(\mathbf{p})$ associated with μ (resp., an eigenvector of $d\mathbf{\Phi}(\mathbf{p})$ associated with λ). For simplicity throughout the entire paper, we will focus on the construction of the unstable manifold. For the case study under consideration, the stable manifold can be obtained by constructing the unstable manifold of the same fixed/periodic point for the inverse map which is also a hybrid map.

Let $\mathcal{N}_{\mathbf{p}}$ be a small neighborhood of $\mathbf{p}$. The local unstable manifold associated to $\mathbf{p}$ (and relative to $\mathcal{N}_{\mathbf{p}}$) is defined as

$$\mathbf{W}_{u,\mathrm{loc}} = \{\mathbf{q} \,|\, \mathbf{\Phi}^{-n}(\mathbf{q}) \in \mathcal{N}_{\mathbf{p}}, \forall\, n \geq 0\}.$$

We then deduce the global unstable manifold associated to $\mathbf{p}$ by writing

$$\mathbf{W}_u = \bigcup_{n \geq 0} \mathbf{\Phi}^n(\mathbf{W}_{u,\mathrm{loc}}).$$

To keep the notations simple we shall denote by $\mathbf{W}_{u,\mathrm{loc}}$ both the local unstable manifold and our chosen parametrization. This latter takes the form

$$\mathbf{W}_{u,\mathrm{loc}}(s) = \sum_{j=0}^{\infty} s^j \mathbf{w}_j, \quad |s| \leq s_0, \tag{5}$$

where $s_0 > 0$, and where

$$\mathbf{w}_0 = \mathbf{p}, \quad \mathbf{w}_1 = \mathbf{U}_+^T = (\mathrm{U}_{+,1}, \mathrm{U}_{+,2}) \tag{6}$$

and

$$\mathbf{W}_{u,\mathrm{loc}}(s) = \mathbf{\Phi}(\mathbf{W}_{u,\mathrm{loc}}(\mu^{-1}s)), \quad |s| \leq \mu s_0. \tag{7}$$

2.1. *The parameterization method*

In this subsection, we briefly review the Parameterization Method for analytic maps which is a functional analytic framework for computing and analyzing invariant manifolds. We first recall the Parameterization Method as it applies to analytic maps defined by explicitly known formulas. Then, we describe some adaptations of this method which are necessary in order to deal with hybrid maps in general.

In the classical setting for the Parameterization Method, $\mathbf{\Phi}$ is explicitly defined as a function of the variables (x, y). Assume that $\mathbf{\Phi}$ admits the following asymptotic

$$\mathbf{\Phi}(x,y) = \sum_{(i,j)\in\mathbb{N}^2} x^i y^j \mathbf{\Lambda}_{i,j},$$
$$\text{where } \mathbf{\Lambda}_{i,j} = (\Lambda_{i,j,1}, \Lambda_{i,j,2}).$$

The technique consists of following an inductive power matching method: by identifying terms on the left-hand side of Eq. (7) with the terms on the right-hand side, one deduces the $\mathbf{w}_j$'s for $j \geq 2$ by induction on j. Observe that since we are considering an analytic map, the expansion of the unstable manifold converges for all $|t| < \rho$ for some $\rho > 0$. The expansion is unique up to a linear rescaling in the variable t. See for instance [Franceschini & Russo, 1981; Krauskopf *et al.*, 2005; Lu *et al.*, 2016; James, 2020] for more examples, details and discussions. A similar approach can be followed in the case our search is for the unstable manifold of an analytic vector field, see [Lessard *et al.*, 2014; Lessard *et al.*, 2011; Lu *et al.*, 2016].

In this work, we consider a hybrid map defined by $\mathbf{\Phi} = \mathbf{L} \circ \mathcal{X}_\tau$. Since $\mathcal{X}$, is analytic, $\mathbf{\Phi}$ defines an analytic map so the Parameterization Method is a reasonable tool to employ. However, it is in general difficult to work out the asymptotics of $\mathbf{\Phi} = \mathbf{L} \circ \mathcal{X}_\tau$ by hand via formal computations as described above especially if the time τ cannot be chosen small (see Sec. 3 for more details). The power matching technique described above is not realistic and our approach needs to be different.

We first assume that we know the locus of a fixed (or periodic) point $\mathbf{p}$ of saddle type and we also know the eigenvalues λ and μ of $d\mathbf{\Phi}(\mathbf{p})$ and with their corresponding eigenspaces defined in Eq. (4). Section 3 is devoted to address this question for our case study, i.e. the van der Pol hybrid map. We now express $\mathbf{\Phi}$ near the hyperbolic fixed point $\mathbf{p}$. Let $d_1 > 0$ and $d_2 > 0$ and define

$$\begin{aligned} &\mathbf{T} : R_2 \to \mathbb{R}^2, \\ &(x,y) \mapsto \mathbf{T}(x,y) = \mathbf{p} + x\mathbf{U}_+ + y\mathbf{U}_-, \end{aligned} \tag{8}$$

where $R_2 = [-d_2, d_2] \times [-d_1, d_1]$ and

$$\boldsymbol{\phi} : R_2 \to \mathbb{R}^2, \quad (x,y) \mapsto \mathbf{T}^{-1} \circ \mathbf{\Phi} \circ \mathbf{T}(x,y). \tag{9}$$

After an additional linear rescaling in (x, y) one may assume that $d_2 = 2$ and $d_1 = 1$. In this new system of coordinates, the x-axis coincides with the unstable direction of the linearization of $\boldsymbol{\phi}$ at the origin and the y-axis with that of the stable direction. Furthermore, a parametrization of the unstable manifold of ϕ at the origin can be written as follows

$$\mathcal{W}(s) = (s + s^2\mathcal{W}_1(s), \mathcal{W}_2(s)), \quad |s| \leq s_0,$$

where $s_0 > 0$, both $\mathcal{W}_1$ and $\mathcal{W}_2$ are analytic functions. Let $\kappa > 0$. By putting $s = \kappa t$, and taking κ sufficiently small the above parametrization writes

$$\mathcal{W}(\kappa t) = \mathbf{W}(t) = (\kappa t + t^2 h_1^*(t), h_2^*(t)), \quad |t| \leq 1,$$

where for all $|t| \leq 1$,

$$\begin{aligned} &|h_1^*|(t) \leq \kappa, \quad |h_2^*|(t) \leq \kappa, \\ &\left|\frac{dh_1^*}{dy}\right|(t) \leq 1, \quad \left|\frac{dh_2^*}{dy}\right| \leq 1. \end{aligned}$$

Since $\boldsymbol{\phi}$ is analytic, the constant κ is also proportional to the radius of convergence of the expansion of the unstable manifold, (see for instance [Cabré *et al.*, 2003, 2005; Gonzalez & James, 2017; Haro & de la Llave, 2006; Lessard *et al.*, 2015]). We will choose κ in such a way that the radius of convergence of the ensuing expansion is at least 2.

In Sec. 2.2, we construct a space of vector-valued functions satisfying the above inequalities

and a contracting operator on that space. Thanks to (6), $\mathbf{W}$ satisfies

$$\mathbf{W}(t) = \boldsymbol{\phi}(\mathbf{W}(\mu^{-1}t)), \quad |t| \leq 1,$$

it will be clear, from the definition, that $\mathbf{h}^* = (h_1^*, h_2^*)$ is a fixed point of that operator.

Before introducing the operator, we need to set up some preliminaries. Write $\boldsymbol{\phi}(x,y) = (\boldsymbol{\phi}_1(x,y), \boldsymbol{\phi}_2(x,y))$. We have

$$\begin{aligned} \boldsymbol{\phi}_1(x,y) &= \mu x + H_1(x,y), \\ \boldsymbol{\phi}_2(x,y) &= \lambda y + H_2(x,y), \end{aligned} \tag{10}$$

where H_1 and H_2 represent the higher order terms. In the present context those higher order terms are unknown. However, we have the following estimates: both H_1 and H_2 are written as

$$H_i(x,y) = x^2 H_{i1}(x) + y H_{i2}(x,y), \quad i = 1,2, \tag{11}$$

where the H_{i1}'s ($i = 1$ or 2) are analytic and one may assume that there exists $M > 0$ such that for all $(x,y) \in R_2$

$$\begin{aligned} &|H_{i1}(x)| \leq M, \quad |H_{i1}'(x)| \leq M, \\ &|H_{i2}(x,y)| \leq M|x| + M|y|, \\ &\qquad \text{and} \\ &\left|\frac{\partial H_{i1}}{\partial x}(x,y)\right| \leq M, \\ &\left|\frac{\partial H_{i2}}{\partial x}(x,y)\right| \leq M. \end{aligned} \tag{12}$$

Let $0 < X_1 \leq 2$ and $0 < Y_1 \leq 1$ and let

$$R_{X_1,Y_1} = [-X_1, X_1] \times [-Y_1, Y_1].$$

Define

$$\begin{aligned} \mathbf{A} &= \sup_{(x,y)\in R_{X_1,Y_1}} \left|\frac{\partial \boldsymbol{\phi}_1}{\partial x}(x,y)\right|, \\ \mathbf{B} &= \sup_{(x,y)\in R_{X_1,Y_1}} \left|\frac{\partial \boldsymbol{\phi}_1}{\partial y}(x,y)\right|, \\ \mathbf{C} &= \sup_{(x,y)\in R_{X_1,Y_1}} \left|\frac{\partial \boldsymbol{\phi}_2}{\partial x}(x,y)\right|, \\ \mathbf{D} &= \sup_{(x,y)\in R_{X_1,Y_1}} \left|\frac{\partial \boldsymbol{\phi}_2}{\partial y}(x,y)\right|. \end{aligned} \tag{13}$$

Thanks to Eqs. (10)–(12), we have

$$\begin{cases} \mathbf{A} \leq |\mu| + M(2X_1 + X_1^2 + Y_1), \\ \mathbf{B} \leq MX_1 + 2MY_1, \\ \mathbf{C} \leq M(2X_1 + X_1^2 + Y_1), \\ \mathbf{D} \leq |\lambda| + MX_1 + 2MY_1. \end{cases} \tag{14}$$

We also assume that $|\mu|^{-1} < 1/3$. The latter condition is probably not necessary but is easily achieved by replacing $\boldsymbol{\phi}$ by $\boldsymbol{\phi}^\ell$ for ℓ sufficiently large. A fixed point for $\boldsymbol{\phi}$ is still a fixed point for $\boldsymbol{\phi}^\ell$ with the same invariant manifold, μ^ℓ being the new unstable eigenvalue. We choose κ sufficently small such that

$$\begin{aligned} &|\mu|^{-2} + 34\kappa M|\mu|^{-3} < 1, \\ &|\mu|^{-1} + 7\kappa M|\mu|^{-2} < \frac{1}{2}, \\ &|\mu|^{-1} + 9\kappa M|\mu|^{-3} < \frac{1}{3} \end{aligned} \tag{15}$$

and we now define the appropriate set of vector-valued functions.

2.2. *A first fixed point operator*

In this subsection, we introduce an appropriate space, and a nonlinear operator on this space which will characterize parameterizations of the unstable manifold. Let

$$\begin{aligned} \mathbf{C}^1([-1,1]) = \{&\mathbf{g} : [-1,1] \to \mathbb{R}^2, \\ &t \mapsto (g_1(t), g_2(t)), \mathbf{g} \text{ being } \mathbf{C}^1\}. \end{aligned}$$

Let $\mathbf{f}, \mathbf{h}$ be two elements in $\mathbf{C}^1([-1,1])$ and write

$$\mathbf{f} = (h_1(t), h_2(t)), \quad \mathbf{h}(t) = (h_1(t), h_2(t)).$$

The set $\mathbf{C}^1([-1,1])$ is equipped with the following metric

$$\begin{aligned} \mathbf{d}(\mathbf{f},\mathbf{h}) = \max\Bigg\{ &\sup_{|t|\leq 1} |f_1(t) - h_1(t)|, \\ &\sup_{|t|\leq 1} |f_2(t) - h_2(t)| \Bigg\}. \end{aligned}$$

Let $b > 1$. We say that $\mathbf{f} = (f_1, f_2) \in \mathbf{C}_b^1([-1,1]) \subset \mathbf{C}^1([-1,1])$ if

$$\begin{aligned} &|f_1(t)| \leq \kappa, \quad |f_2(t)| \leq \kappa, \\ &|f_1'(t)| \leq b, \quad |f_2'(t)| \leq b, \quad \forall\, t \in [-1,1]. \end{aligned} \tag{16}$$

Observe that if $\mathbf{f} \in \mathbf{C}^1_b([-1,1])$, thanks to the above condition and the Mean Value theorem, both components f_1 and f_2 are b-Lipschitz, i.e. we have

$$\|\mathbf{f}(t) - \mathbf{f}(s)\| \leq b\,|t-s| \quad \forall\, s,t \in [-1,1],$$

where

$$\|f(t)\| = \max\{|f_1|(t), |f_2|(t)\}.$$

We also define the following map

$$\mathbf{J} : \mathbf{C}^1_b([-1,1]) \to \mathbf{C}^1([-1,1]), \quad \mathbf{f} \mapsto \mathbf{J}(\mathbf{f}) = \mathbf{C}_{\mathbf{f}},$$

where

$$\mathbf{C}_{\mathbf{f}}(t) = (C_{\mathbf{f},1}(t), C_{\mathbf{f},2}(t)) = (\kappa t + t^2 f_1(t), t^2 f_2(t)).$$

We now define an appropriate operator, $\psi : \mathbf{C}^1_b([-1,1]) \to \mathbf{C}^1_b([-1,1])$, such that $\mathbf{h}$ is a stable fixed point of ψ. In what follows $R_\mu(t) = \mu^{-1}t$. We first state the following lemma.

Lemma 1. *Let $b > 1$ and $\mathbf{f} \in \mathbf{C}^1_b([-1,1])$. There exists $L_{\mathbf{f}} \in \mathbf{C}^1_b([-1,1])$, $L_{\mathbf{f}} = (L_{\mathbf{f},1}, L_{\mathbf{f},2})$ such that*

$$\begin{aligned}\boldsymbol{\phi} \circ \mathbf{J}(\mathbf{f}) \circ R_\mu(t) &= (\kappa t + t^2 L_{\mathbf{f},1}(t), t^2 L_{\mathbf{f},2}(t)) \\ &= \mathbf{J}(L_{\mathbf{f}}).\end{aligned}$$

Proof. Write

$$\mathbf{C}_{\mathbf{f}}(t) = (\kappa t + t^2 f_1(t), t^2 f_2(t)) = (tV_1(t), t^2 V_2(t)),$$

where $V_1(t) = \kappa + t f_1(t)$ and $V_2(t) = f_2(t)$. From Eq. (16), we have

$$\begin{aligned}&|V_1(t)| \leq 2\kappa, \quad |V_2(t)| \leq \kappa, \\ &|V_1'(t)| \leq \kappa + b, \quad |V_2'(t)| \leq b.\end{aligned} \tag{17}$$

Let $u \in [-1,1]$. We write

$$\begin{aligned}H_1(uV_1(u), u^2 V_2(u)) &= u^2 \overline{H}_1(u), \\ H_2(uV_1(u), u^2 V_2(u)) &= u^2 \overline{H}_2(u).\end{aligned} \tag{18}$$

From Eq. (11) we have

$$\begin{aligned}\overline{H}_1(u) &= V_1^2(u) H_{11}(uV_1(u)) \\ &\quad + V_2(u) H_{12}(uV_1(u), u^2 V_2(u)) \\ \overline{H}_2(u) &= V_1^2(u) H_{21}(uV_1(u)) \\ &\quad + V_2(u) H_{22}(uV_1(u), u^2 V_2(u))\end{aligned}$$

From Eqs. (12) and (17) we have

$$|\overline{H}_i(u)| \leq 7\kappa^2 M, \quad i = 1,2. \tag{19}$$

Moreover, for all $|u| \leq 1$ we have

$$\begin{aligned}\overline{H}_i'(u) &= 2V_1(u)V_1'(u)H_{i1}(uV_1(u)) \\ &\quad + V_2'(u)H_{i2}(uV_1(u), u^2V_2(u)) \\ &\quad + V_1^2(u)(V_1(u) + uV_1'(u))H_{i1}'(uV_1(u)) \\ &\quad + V_2(u)(V_1(u) + uV_1'(u)) \\ &\quad \times \frac{\partial H_{i2}}{\partial x}(uV_1(u), u^2V_2(u)) \\ &\quad + V_2(u)(2uV_2(u) + u^2V_2'(u)) \\ &\quad \times \frac{\partial H_{i2}}{\partial y}(uV_1(u), u^2V_2(u)), \quad i = 1,2.\end{aligned}$$

Thanks again to Eqs. (12) and (17), for all $|u| \leq 1$ we have

$$|\overline{H}_i'(u)| \leq \kappa \mathbf{K}_b M \quad i = 1,2, \tag{20}$$

where

$$\begin{aligned}\mathbf{K}_b &= 4(\kappa + b) + 3b + (4\kappa + 1)(3\kappa + b) + (2\kappa + b) \\ &= 9b + 4\kappa b + 9\kappa + 12\kappa^2.\end{aligned}$$

Since $\kappa \leq 1 \leq \mathbf{b}$ we have

$$\mathbf{K}_b \leq 34b. \tag{21}$$

Write $\mathbf{f}(t) = (f_1(t), f_2(t))$ as above and write

$$\boldsymbol{\phi} \circ \mathbf{J}(\mathbf{f}) \circ \mathrm{R}_\mu(t) = (F_1(t), F_2(t)),$$

where

$$\begin{aligned}F_1(t) &= \boldsymbol{\phi}_1(\kappa\mu^{-1}t + \mu^{-2}t^2 f_1(\mu^{-1}t), \mu^{-2}t^2 f_2(\mu^{-1}t)), \\ F_2(t) &= \boldsymbol{\phi}_2(\kappa\mu^{-1}t + \mu^{-2}t^2 f_1(\mu^{-1}t), \mu^{-2}t^2 f_2(\mu^{-1}t)).\end{aligned} \tag{22}$$

Replacing u by $\mu^{-1}t$ in Eq. (18) and thanks to Eq. (10) we have

$$\begin{aligned}F_1(t) &= \kappa t + \mu^{-1}t^2 f_1(\mu^{-1}t) \\ &\quad + H_1(\mu^{-1}t + \mu^{-2}t^2 f_1(\mu^{-1}t), \mu^{-2}t^2 f_2(\mu^{-1}t)) \\ &= \kappa t + \mu^{-1}t^2 f_1(\mu^{-1}t) + \mu^{-2}t^2 \overline{H}_1(\mu^{-1}t) \\ &= \kappa t + t^2 L_{\mathbf{f},1}(t),\end{aligned} \tag{23}$$

$$\begin{aligned}F_2(t) &= \lambda\mu^{-2}t^2 f_2(\mu^{-1}t)\\ &\quad + H_2(\mu^{-1}t + \mu^{-2}t^2 f_1(\mu^{-1}t), \mu^{-2}t^2 f_2(\mu^{-1}t))\\ &= \lambda\mu^{-2}t^2 f_2(\mu^{-1}t) + \mu^{-2}t^2\overline{H}_2(\mu^{-1}t)\\ &= t^2 L_{\mathbf{f},2}(t) \end{aligned} \tag{24}$$

where

$$\begin{aligned}L_{\mathbf{f},1}(t) &= \mu^{-1}f_1(\mu^{-1}t) + \mu^{-2}\overline{H}_1(\mu^{-1}t),\\ L_{\mathbf{f},2}(t) &= \lambda\mu^{-2}f_2(\mu^{-1}t) + \mu^{-2}\overline{H}_2(\mu^{-1}t).\end{aligned} \tag{25}$$

We need to show that both $L_{\mathbf{f},1}(t)$ and $L_{\mathbf{f},2}(t)$ satisfy Eq. (16). Since $\mathbf{f}$ satisfies Eq. (16), with Eqs. (15) and (19), we have

$$\begin{aligned}|L_{\mathbf{f},1}(t)| &\le \kappa|\mu^{-1}| + 7\kappa^2 M|\mu^{-2}| < \frac{\kappa}{2},\\ |L_{\mathbf{f},2}(t)| &\le \kappa|\lambda||\mu^{-2}| + 7\kappa^2 M|\mu^{-2}| < \frac{\kappa}{2}.\end{aligned} \tag{26}$$

Also, from Eq. (25) and thanks to Eqs. (15), (20) and (21) we have

$$\begin{aligned}|L'_{\mathbf{f},1}(t)| &\le |\mu^{-2}|b + 34\kappa bM|\mu^{-3}| < b,\\ |L'_{\mathbf{f},2}(t)| &\le |\lambda||\mu^{-2}|b + 34\kappa bM|\mu^{-3}| < b,\end{aligned} \tag{27}$$

which completes the proof of Lemma 1. ■

Thanks to Lemma 1, we can define the following operator

$$\begin{aligned}\psi : \mathbf{C}^1_b([-1,1]) &\to \mathbf{C}^1_b([-1,1]),\\ \mathbf{f} &\mapsto \mathbf{J}^{-1}\circ\boldsymbol{\phi}\circ\mathbf{J}(\mathbf{f})\circ \mathrm{R}_\mu = L_{\mathbf{f}}\end{aligned}$$

and we state the following proposition.

Proposition 1. *Assume* $|\mu|^{-1} < 1/3$ *and* κ *satisfies Eq. (15). For all* $\mathbf{f}, \mathbf{g} \in \mathbf{C}^1_b([-1,1])$

$$\mathbf{d}(\psi(\mathbf{f}), \psi(\mathbf{g})) \le \frac{1}{3}\mathbf{d}(\mathbf{f}, \mathbf{g}).$$

We want to emphasize here that $\mathbf{h}^*$ introduced in Sec. 2.1 is a fixed point of this operator.

Proof. Take $\mathbf{f}$ as above. Write $\mathbf{g}(t) = (g_1(t), g_2(t))$ where $\mathbf{g}$ satisfies Eq. (16). Following the same computation we did above for $\mathbf{f}$, and recalling Eq. (22), we have

$$\begin{aligned}\boldsymbol{\phi}\circ\mathbf{J}\circ\mathbf{f}\circ\mathrm{R}_\mu(t) &= (F_1(t), F_2(t)),\\ \boldsymbol{\phi}\circ\mathbf{J}\circ\mathbf{g}\circ\mathrm{R}_\mu(t) &= (G_1(t), G_2(t)),\end{aligned}$$

where

$$\begin{aligned}G_1(t) &= \kappa t + t^2 L_{\mathbf{g},1}(t)\\ &= \boldsymbol{\phi}_1(\kappa\mu^{-1}t + \mu^{-2}t^2 g_1(\mu^{-1}t), \mu^{-2}t^2 g_2(\mu^{-1}t)),\\ G_2(t) &= t^2 L_{\mathbf{g},2}(t)\\ &= \boldsymbol{\phi}_2(\kappa\mu^{-1}t + \mu^{-2}t^2 g_1(\mu^{-1}t), \mu^{-2}t^2 g_2(\mu^{-1}t)).\end{aligned} \tag{28}$$

We need to show that

$$\begin{aligned}&\max\left\{\sup_{|t|\le1}|L_{\mathbf{f},1}(t) - L_{\mathbf{g},1}(t)|, \sup_{|t|\le1}|L_{\mathbf{f},2}(t) - L_{\mathbf{g},2}(t)|\right\}\\ &\quad\le \frac{1}{3}\max\left\{\sup_{|t|\le1}|f_1(t) - g_1(t)|,\right.\\ &\qquad\left.\sup_{|t|\le1}|f_2(t) - g_2(t)|\right\}\\ &\quad= \frac{1}{3}\mathbf{d}(\mathbf{f}, \mathbf{g}).\end{aligned} \tag{29}$$

Observe that for all $|t| \le 1$, we have

$$\begin{aligned}&|\kappa\mu^{-1}t + \mu^{-2}t^2 f_1(\mu^{-1}t)| \le 2\kappa|\mu|^{-1},\\ &|\mu^{-2}t^2 f_2(\mu^{-1}t)| \le \kappa|\mu|^{-2},\\ &|\kappa\mu^{-1}t + \mu^{-2}t^2 g_1(\mu^{-1}t)| \le 2\kappa|\mu|^{-1},\\ &|\mu^{-2}t^2 g_2(\mu^{-1}t)| \le \kappa|\mu|^{-2},\end{aligned}$$

which implies that both $\mathbf{J}\circ\mathbf{f}\circ R_\mu(t)$ and $\mathbf{J}\circ\mathbf{g}\circ R_\mu(t)$ belong to the rectangle

$$\begin{aligned}R_{X_1,Y_1} &= [-X_1, X_1]\times[-Y_1, Y_1],\\ &\text{where } X_1 = 2\kappa|\mu|^{-1},\ \ Y_1 = \kappa|\mu|^{-2}.\end{aligned} \tag{30}$$

From (14) it follows that

$$\begin{cases}\mathbf{A} \le |\mu| + M|\mu|^{-1}(4\kappa + 4\kappa^2|\mu|^{-1} + \kappa|\mu|^{-1})\\ \quad\le |\mu| + 9\kappa M|\mu|^{-1}\\ \mathbf{B} \le 2\kappa M(|\mu|^{-1} + |\mu|^{-2}|) \le 4\kappa M|\mu|^{-1}\\ \mathbf{C} \le M|\mu|^{-1}(4\kappa + 4\kappa^2|\mu|^{-1} + \kappa|\mu|^{-1})\\ \quad\le 9\kappa M|\mu|^{-1}\\ \mathbf{D} \le |\lambda| + 2\kappa M(|\mu|^{-1} + |\mu|^{-2})\\ \quad\le |\lambda| + 4\kappa M|\mu|^{-1}\end{cases} \tag{31}$$

From Eqs. (13), (22)–(24), (28) and (30), we have

$$\begin{aligned}&|F_1(t) - G_1(t)|\\ &\quad = |t^2 L_{\mathbf{f},1}(t) - t^2 L_{\mathbf{g},1}(t)|\\ &\quad \le |\mu|^{-2}\mathbf{A}t^2|f_1(\mu^{-1}t) - g_1(\mu^{-1}t)|\\ &\qquad + |\mu|^{-2}\mathbf{B}t^2|f_2(\mu^{-1}t) - g_2(\mu^{-1}t)| \qquad (32)\end{aligned}$$

and

$$\begin{aligned}&|F_2(t) - G_2(t)|\\ &\quad = |t^2 L_{\mathbf{f},2}(t) - t^2 L_{\mathbf{g},2}(t)|\\ &\quad \le \mu^{-2}\mathbf{C}t^2|f_1(\mu^{-1}t) - g_1(\mu^{-1}t)|\\ &\qquad + \mu^{-2}\mathbf{D}t^2|f_2(\mu^{-1}t) - g_2(\mu^{-1}t)|. \qquad (33)\end{aligned}$$

Therefore from Eqs. (31)–(33), we have

$$\begin{aligned}&|L_{\mathbf{f},1}(t) - L_{\mathbf{g},1}(t)|\\ &\quad \le |\mu|^{-2}(|\mu| + 9\kappa M|\mu^{-1}|)\\ &\qquad \times |f_1(\mu^{-1}t) - g_1(\mu^{-1}t)|\\ &\qquad + |\mu|^{-2}(4\kappa M|\mu|^{-1})|f_2(\mu^{-1}t) - g_2(\mu^{-1}t)| \qquad (34)\end{aligned}$$

and

$$\begin{aligned}&|L_{\mathbf{f},2}(t) - L_{\mathbf{g},2}(t)|\\ &\quad \le \mu|^{-2}(9\kappa M|\mu^{-1}|)|f_1(\mu^{-1}t) - g_1(\mu^{-1}t)|\\ &\qquad + |\mu|^{-2}(|\lambda| + 4\kappa M|\mu|^{-1})\\ &\qquad \times |f_2(\mu^{-1}t) - g_2(\mu^{-1}t)|. \qquad (35)\end{aligned}$$

Since

$$\begin{aligned}4\kappa M|\mu|^{-1} &< 9\kappa M|\mu|^{-1} < |\lambda| + 9\kappa M|\mu|^{-1}\\ &< |\mu| + 9\kappa M|\mu|^{-1},\end{aligned}$$

for all $-1 \le t \le 1$ we have

$$\begin{aligned}&|L_{\mathbf{f},1}(t) - L_{\mathbf{g},1}(t)|\\ &\quad \le |\mu|^{-2}(|\mu| + 9\kappa M|\mu|^{-1})\mathbf{d}(\mathbf{f},\mathbf{g}) \qquad (36)\end{aligned}$$

and

$$\begin{aligned}&|L_{\mathbf{f},2}(t) - L_{\mathbf{g},2}(t)|\\ &\quad \le |\mu|^{-2}(|\mu| + 9\kappa M|\mu^{-1}|)\mathbf{d}(\mathbf{f},\mathbf{g}). \qquad (37)\end{aligned}$$

Since μ satisfies Eq. (15), from Eqs. (36) and (37) we finally conclude that

$$\mathbf{d}(\psi(\mathbf{f}), \psi(\mathbf{g})) \le \frac{1}{3}\mathbf{d}(\mathbf{f},\mathbf{g}). \qquad \blacksquare$$

2.3. *Lagrange–Chebyshev interpolation*

Next, we consider the practical problem of numerically computing a fixed point of ψ. Specifically, $\mathbf{C}_b^1([-1,1]$ is infinite dimensional so in order to approximate $\mathbf{W}$ with a computer we must restrict to a finite dimensional subspace and discretize ψ appropriately. We do this by considering a reduced version of ψ defined by restricting to the space of Lagrange–Chebyshev interpolants. We begin by briefly reviewing these interpolants.

Let $b > 1$ and $q \ge 1$ be an integer. We denote by $\mathbb{R}_q[t]$ the set of polynomial functions (in the variable t) of degree less than or equal to $q-1$ and

$$\begin{aligned}\ell_b([-1,1]) = \{&f : [-1,1] \to \mathbb{R},\\ &|f(t) - f(s)| \le b, \forall\, t, s \in [-1,1]\}.\end{aligned}$$

We define the Lagrange–Chebyshev interpolating operator

$$\mathcal{L}_q : \ell_b([-1,1]) \to \mathbb{R}_q[t], \quad h \mapsto \mathcal{L}_q(h),$$

where

$$\mathcal{L}_q(h)(t) = \sum_{j=0}^{q-1} c_j T_j(t), \quad |t| \le 1,$$

where the T_j's are the Chebyshev polynomials of the first kind, i.e.

$$T_j(t) = \cos(j \arccos(t)), \quad j = 0, \ldots, q-1,$$

$$c_j = \frac{2}{q}\sum_{k=0}^{q-1} h(u_k)T_j(u_k), \quad j > 0,$$

$$c_0 = \frac{1}{q}\sum_{k=0}^{q-1} h(u_k),$$

where the u_k's are the Chebyshev nodes on $[-1,1]$, i.e.

$$u_k = \cos\left(\frac{2k+1}{2q}\pi\right), \quad k = 0, \ldots, q-1.$$

For each integer q the above set of nodes will be denoted by

$$\mathbf{N}(q) = \{u_k, k = 0, \ldots, q-1\}.$$

See [Handscomb & Mason, 2002] for more details. Both sets $\ell_b([-1,1])$ and $\mathbb{R}_q[t]$ are equipped with the following norm

$$\|h\|_\infty = \sup_{x\in[-1,1]} |h(t)|.$$

The operator $\mathcal{L}_q$ is linear, and for all $h \in \ell_b([-1,1])$, $\mathcal{L}_q(h)$ converges uniformly to h on $[-1,1]$ as q tends to ∞. More precisely, the following lemma holds.

Lemma 2. *Let $b > 1$ and let $z \in \ell_b([-1,1])$. Then*

$$\|\mathcal{L}_q(z) - z\|_\infty \leq \frac{(1+\mu_q)}{q} b,$$

where

$$\mu_q = \frac{1}{\pi}\sum_{j=0}^{q-1} \cot\left(\frac{\left(j+\frac{1}{2}\right)\pi}{2q}\right) = \frac{2}{\pi}\log(q) + 0.9625 + \mathcal{O}\left(\frac{1}{q}\right).$$

Lemma 2 is a direct consequence of Jackson's Theorem and its Corollary 6.14A in [Handscomb & Mason, 2002]. Both results are formulated for a continuous function h defined on $[-1,1]$ with modulus of continuity

$$m(\delta) = \sup_{|x_1-x_2|\leq\delta} |h(x_1) - h(x_2)|.$$

In the case where h is b-Lipschitz we have

$$m(\delta) \leq b\delta. \tag{38}$$

Corollary 6.14A in [Handscomb & Mason, 2002] states that

$$\|\mathcal{L}_q(z) - z\|_\infty \leq (1+\mu_q) m\left(\frac{1}{q}\right)$$

and from Eq. (38) we have

$$\|\mathcal{L}_q(z) - z\|_\infty \leq \frac{b(1+\mu_q)}{q},$$

from which Lemma 2 follows. Observe that the estimate

$$\mu_q = \frac{2}{\pi}\log(q) + 0.9625 + \mathcal{O}\left(\frac{1}{q}\right)$$

given in [Handscomb & Mason, 2002], implies that

$$\|\mathcal{L}_q(z) - z\|_\infty \to 0 \quad \text{as } q \to \infty$$

independently from the choice of z.

Remark 2.1. Observe that the upper bound for $\|\mathcal{L}_q(z) - z\|_\infty$ given in Lemma 2 is far from being the most optimal one. For instance, following [Handscomb & Mason, 2002], if z is analytic, there exists $M > 0$ and $\tilde{r} > 1$ such that

$$\|\mathcal{L}_q(z) - z\|_\infty \leq \frac{M}{\tilde{r}^q}.$$

In the latter estimate, both constants M and $\tilde{r}$ depend upon the function z, while in the former estimate (given by Lemma 2), the upper bound only depends upon the constant b.

We now define

$$\mathbf{L}_b([-1,1]) = \{\mathbf{h} : [-1,1] \to \mathbb{R}^2, \|\mathbf{h}\| \leq \kappa, \|\mathbf{h}(t_1) - \mathbf{h}(t_2)\| \leq b|t_1 - t_2|, \forall\, t_1, t_2 \in [-1,1]\}$$

and $\mathbf{P}_q([-1,1]) \subset \mathrm{R}_q \times \mathrm{R}_q$ the subspace of vector valued functions (of degree less than or equal to $q-1$) with components bounded by κ on $[-1,1]$. We extend the definition of $\mathcal{L}_q$ to an element of $\mathbf{P}_q([-1,1])$ in the following manner. We write

$$\mathcal{L}_q(\mathbf{f}) = (\mathcal{L}_q(f_1), \mathcal{L}_q(f_2)).$$

Corollary 2.1. *Let $b > 0$ and let $z \in \mathbf{L}_b([-1,1])$. There exists $q_0 = q_0(\mathbf{b})$ such that for all $s \geq q_0$,*

$$\sup_{|t|\leq 1} \|\mathcal{L}_s(z)(t)\| \leq 2 \sup_{|t|\leq 1} \|z(t)\|.$$

Proof. Since $\mathcal{L}_q$ is linear it is sufficient to prove the corollary when $\sup_{|t|\leq 1}\|z(t)\| = 1$. From Lemma 2, choose $q_0 > 0$ sufficiently large such that for all $s > q_0$

$$\frac{(1+\mu_s)b}{s} \leq 1.$$

We have for all $t \in [-1,1]$

$$\|\mathcal{L}_s(z)(t)\| \leq \|\mathcal{L}_s(z)(t) - z(t)\| + \|z(t)\| \leq 2,$$

ending the proof of the corollary. ■

As a consequence, it is important to observe that if $\mathbf{f} \in \mathbf{C}_b^1([-1,1])$ for some $b > 1$, by Eq. (16)

we have

$$\|\mathbf{f}(t)\| \leq \kappa, \quad \forall |t| \leq 1$$

and thanks to Eq. (26) we have

$$\|\psi(\mathbf{f})(t)\| \leq \frac{\kappa}{2}, \quad \forall\, |t| \leq 1.$$

Thanks to Corollary 2.1, we then have

$$\|\mathcal{L}_q \circ \psi(\mathbf{f})(t)\| \leq \kappa, \quad \forall\, |t| \leq 1. \tag{39}$$

By definition, $\mathcal{L}_q \circ \psi(\mathbf{f})$ is a polynomial vector valued function and thus has a bounded derivative on $[-1, 1]$. Equation (39) therefore implies that $\mathcal{L}_q \circ \psi(\mathbf{f}) \in \mathbf{C}^1_{b'}([-1, 1])$ for some $b' \geq b$.

We are now in a position to introduce a new operator that takes the former operator and the interpolation techniques into account.

2.4. *The reduced operator*

We now define the operator which is actually iterated in our computations. This is a restriction of ψ to a finite dimensional subspace spanned by Chebyshev polynomials. We define

$$\psi_q : \mathbf{P}_q([-1, 1]) \to \mathbf{P}_q([-1, 1]), \quad \mathbf{h} \mapsto \mathcal{L}_q \circ \psi(\mathbf{h}).$$

We now state the following proposition.

Proposition 2. *For all $q \geq 1$, $\delta > 0$, and for all $\mathbf{g} \in \mathbf{P}_q([-1, 1], R_1)$ there exists $q_1 \geq q$ such that for all $s \geq q_1$,*

$$d(\psi_s(\mathbf{g}), \psi(\mathbf{g})) \leq \delta.$$

Observe that such q_1 depends upon the choice of q, δ and $\mathbf{g}$.

Corollary 2.2. *For all $q \geq 1$, $\delta > 0$, and for all $\mathbf{g} \in \mathbf{P}_q([-1, 1])$, there exists $q_1 > q$ such that for all $s_1, s_2 \geq q_1$,*

$$d(\psi_{s_1}(\mathbf{g}), \psi_{s_2}(\mathbf{g})) \leq \delta.$$

Proof. It is sufficient to apply Proposition 2, twice. More precisely, let $\delta > 0$ and $\mathbf{g} \in \mathbf{P}_q([-1, 1])$. Choose $s_1 \geq q_1$, $s_2 \geq q_1$ with

$$d(\psi_{s_1}(\mathbf{g}), \psi(\mathbf{g})) \leq \frac{\delta}{2} \quad \text{and}$$

$$d(\psi_{s_2}(\mathbf{g}), \psi(\mathbf{g})) \leq \frac{\delta}{2}.$$

Thanks to the triangular inequality we have

$$d(\psi_{s_1}(\mathbf{g}), \psi_{s_2}(\mathbf{g})) \leq \delta$$

and the corollary follows. ■

Proof of Proposition 2. Let $q \geq 1$ and $\mathbf{g} = (g_1, g_2) \in \mathbf{P}_q([-1, 1])$. Since g_1 and g_2 are polynomial functions, there exists $b \geq 1$ such that $\mathbf{g} \in \mathbf{C}^1_b([-1, 1])$. Write

$$\psi(\mathbf{g})(t) = (G_1(t), G_2(t)).$$

Since

$$|G_1'(t)| \leq b, \quad |G_2'(t)| \leq b,$$

both G_1 and G_2 are b-Lipschitz. Let $\delta > 0$ be given. Thanks to Lemma 2, there exists $q_1 > 1$ such that for all $s \geq q_1$

$$\|\mathcal{L}_s(G_1) - G_1\| \leq \frac{b(1 + \mu_s)}{s} \leq \delta \quad \text{and}$$

$$\|\mathcal{L}_s(G_2) - G_1\| \leq \frac{b(1 + \mu_s)}{s} \leq \delta,$$

which implies that

$$d(\mathcal{L}_s \circ \psi(\mathbf{g}), \psi(\mathbf{g})) = d(\psi_s(\mathbf{g}), \psi(\mathbf{g})) \leq \delta,$$

ending the proof of Proposition 2. ■

Remark 2.2. The estimate given in Lemma 2 (and invoked above in the proof of Proposition 2), reveals that for a given $\delta > 0$, q_1 satisfies

$$\frac{\log(q_1)}{q_1} \sim \delta.$$

For analytic functions, thanks to the constants M and $\tilde{r}$, q_1 can be chosen much smaller (see Remark 2.1 above). However, since we have no information on the value of both M and $\tilde{r}$, our search for such q_1 is numerical. We proceed as follows: for a given $\delta > 0$ and $q > 1$, we choose a set $\mathcal{G}$ of points equally distributed on the interval $[-1, 1]$ consisting of $\sim 100q$ points. For $s \geq q$, we compute

$$\Delta_s = \max_{\xi \in \mathcal{G}} \|\psi(\mathbf{g})(\xi) - \psi_s(\mathbf{g})(\xi)\|$$

and choose q_1 such that $\Delta_{q_1} \leq \delta$ and we verify that $\Delta_s \leq \delta$ for $s > q_1$.

Theorem 1. *Let $q \geq 1$ and $\mathbf{f}$, $\mathbf{g} \in \mathbf{P}_q([-1, 1])$. There exists $q_2 \geq q$ such that for all $s \geq q_2$*

$$\mathbf{d}(\psi_s(\mathbf{f}), \psi_s(\mathbf{g})) \leq \frac{2}{3}\mathbf{d}(\mathbf{f}, \mathbf{g}).$$

Observe again, as in Proposition 2, that q_2 depends upon $q, \delta, \mathbf{f}$ and $\mathbf{g}$.

Proof. Let $\mathbf{f}$, $\mathbf{g} \in \mathbf{P}_q([-1,1])$ and let $b \geq 1$ such that both $\mathbf{f}$ and $\mathbf{g}$ belong to $\mathbf{C}^1_b([-1,1])$. Using the same notation as in Sec. 2.2, we write

$$\psi(\mathbf{f})(t) = (L_{\mathbf{g},1}(t), L_{\mathbf{f},2}(t)),$$
$$\psi(\mathbf{g})(t) = (L_{\mathbf{f},1}(t), L_{\mathbf{g},2}(t)).$$

Recall that both $\psi(\mathbf{f})$ and $\psi(\mathbf{g})$ belong to $\mathbf{C}^1_b([-1,1])$. We already know from Proposition 1 that

$$|L_{\mathbf{f},1}(t) - L_{\mathbf{g},1}(t)| \leq \frac{1}{3}\mathbf{d}(\mathbf{f},\mathbf{g}) \quad \text{and}$$
$$|L_{\mathbf{f},2}(t) - L_{\mathbf{g},2}(t)| \leq \frac{1}{3}\mathbf{d}(\mathbf{f},\mathbf{g}).$$

Let $q_2 = q_0(b)$ given in Corollary 2.1 and $s \geq q_2$. Since $\mathcal{L}_s$ is linear and thanks to Corollary 2.1, we have for $i = 1, 2$

$$\begin{aligned}
&|\mathcal{L}_s(L_{\mathbf{f},i}(t)) - \mathcal{L}_s(L_{\mathbf{g},i}(t))| \\
&\quad = |(\mathcal{L}_s(L_{\mathbf{f},i}(t) - L_{\mathbf{g},i}(t))| \\
&\quad \leq 2|L_{\mathbf{f},i}(t) - L_{\mathbf{g},i}(t)| \\
&\quad \leq \frac{2}{3}\mathbf{d}(\mathbf{f},\mathbf{g}),
\end{aligned}$$

which completes the proof. ■

From now on and up to the end of this section, we assume that we know how to estimate the map $\boldsymbol{\phi}$ in a finite set of points with any desired precision. For the hybrid map under consideration in this paper, see Sec. 3 and the estimate given in Eq. (54).

2.5. *Computing the reduced operator on a set of nodes*

For each integer s we need to compute the image of operator ψ_s on an element $\mathbf{f} \in \mathbf{C}^1_b([-1,1])$ for some $b > 1$. It will be clear in what follows that s will need to be even. Recall that for each integer $s \geq 1$,

$$\mathbf{N}(s) = \left\{ u_k = \cos\left(\frac{2k+1}{2s}\pi\right), k = 0, \ldots, s-1 \right\}.$$

Let s be an even integer and $\mathbf{f} = (f_1, f_2)$ as above. For each $u_k \in \mathbf{N}(s)$, we compute

$$\begin{aligned}
&\boldsymbol{\phi} \circ \mathbf{J} \circ \mathbf{f} \circ R_\mu(u_k) \\
&\quad = \boldsymbol{\phi}(\kappa\mu^{-1}u_k + \mu^{-2}u_k^2 f_1(\mu^{-1}u_k), \\
&\qquad \mu^{-2}u_k^2 f_2(\mu^{-1}u_k)) \\
&\quad = (F_1(u_k), F_2(u_k)), \quad k = 0, \ldots, s-1.
\end{aligned}$$

According to Eqs. (23) and (24) we have

$$F_1(u_k) = \kappa u_k + u_k^2 L_{\mathbf{f},1}(u_k),$$
$$F_2(u_k) = u_k^2 L_{\mathbf{f},1}(u_k).$$

Recall that

$$\Psi(\mathbf{f})(t) = (L_{\mathbf{f},1}(t), L_{\mathbf{f},2}(t)).$$

Since s is even, $0 \notin \mathbf{N}(s)$. Therefore, for each $k = 0, \ldots, s-1$, we may compute

$$L_{\mathbf{f},1}(u_k) = \frac{1}{u_k^2}(F_1(u_k) - \kappa u_k),$$
$$L_{\mathbf{f},2}(u_k) = \frac{F_2(u_k)}{u_k^2}.$$

We then compute

$$\mathcal{L}_s(L_{\mathbf{f},1})(t) = \sum_{j=0}^{s-1} c_j(L_{\mathbf{f},1})T_j(t), \quad |t| \leq 1$$

and

$$\mathcal{L}_s(L_{\mathbf{f},2})(t) = \sum_{j=0}^{s-1} c_j(L_{\mathbf{f},2})T_j(t), \quad |t| \leq 1,$$

where

$$c_j(L_{\mathbf{f},1}) = \frac{2}{s}\sum_{k=0}^{s-1} L_{\mathbf{f},1}(u_k)T_j(u_k), \quad j > 0,$$

$$c_0(L_{\mathbf{f},1}) = \frac{1}{s}\sum_{k=0}^{s-1} L_{\mathbf{f},1}(u_k)$$

and

$$c_j(L_{\mathbf{f},2}) = \frac{2}{s}\sum_{k=0}^{s-1} L_{\mathbf{f},2}(u_k)T_j(u_k), \quad j > 0,$$

$$c_0(L_{\mathbf{f},2}) = \frac{1}{s}\sum_{k=0}^{s-1} L_{\mathbf{f},2}(u_k).$$

2.6. *Construction of a converging sequence*

We first state the following lemma.

Lemma 3. *Let $\nu > 0$ and $(\mathbf{a}_n)$ be a sequence of non-negative real number that satisfies*

$$\mathbf{a}_{m+1} \leq \left(\frac{2}{3}\right)\mathbf{a}_m + \left(\frac{2}{3}\right)^m \nu, \quad m \geq 0.$$

Then, for all integer n, m we have

$$\sum_{j=n}^{m+n} \mathbf{a}_j \leq 3\mathbf{a}_0 \left(\frac{2}{3}\right)^n + \nu\omega_n,$$

where

$$\omega_n = \sum_{j=n}^{\infty} j \left(\frac{2}{3}\right)^{j-1}.$$

Observe that $\omega_n \to 0$, as $n \to \infty$ and therefore $(\sum_{j=0}^{n} \mathbf{a}_j)$ is a Cauchy sequence.

Proof. Since for $m \geq 1$,

$$\mathbf{a}_m \leq \frac{2}{3}\mathbf{a}_{m-1} + \left(\frac{2}{3}\right)^{m-1} \nu,$$

we have that

$$\begin{aligned}\mathbf{a}_m &\leq \frac{2}{3}\left[\frac{2}{3}\mathbf{a}_{m-2} + \left(\frac{2}{3}\right)^{m-2}\nu\right] + \left(\frac{2}{3}\right)^{m-1}\nu \\ &\leq \left(\frac{2}{3}\right)^2 \mathbf{a}_{m-2} + 2\left(\frac{2}{3}\right)^{m-1}\nu\end{aligned}$$

and a straightforward computation gives

$$\mathbf{a}_m \leq \left(\frac{2}{3}\right)^m \mathbf{a}_0 + m\left(\frac{2}{3}\right)^{m-1}\nu, \quad \forall\, m \geq 0$$

and therefore we have

$$\sum_{j=n}^{m+n} \mathbf{a}_j \leq \mathbf{a}_0 \left(\frac{2}{3}\right)^n \sum_{j=0}^{m} \left(\frac{2}{3}\right)^j + \nu \sum_{j=n}^{m+n} j\left(\frac{2}{3}\right)^{j-1}$$

$$\sum_{j=n}^{m+n} \mathbf{a}_j \leq 3\mathbf{a}_0 \left(\frac{2}{3}\right)^n + \nu\omega_n,$$

ending the proof of Lemma 3. ■

Recall that $\mathbf{h}^*$ defined in Sec. 2.1 is the fixed point of ψ and we have

$$\mathbf{C}_{\mathbf{h}^*}(t) = \mathbf{W}(t) = (\kappa t + t^2 h_1^*(t), t^2 h_2^*(t)).$$

Our goal is to estimate $\mathbf{h}^*$ and keep control of the errors. Recall that we know how to compute $\boldsymbol{\phi}$ on a finite set of points. The idea is to mimic ψ by ψ_q for some integer q, this latter integer being subject to change.

Let $\nu > 0$ be a small real number representing the tolerance of our computation. Let $\kappa = 1/10$. As mentioned in Sec. 2.1, the choice of κ determines the radius of convergence of the expansion we are looking for. Therefore, in the same spirit as in the classical parameterization method [van den Berg *et al.*, 2011; Cabré *et al.*, 2003, 2005; Gonzalez & James, 2017; Haro & de la Llave, 2006; Lessard *et al.*, 2015], we may need to redo the procedure described below with different values of κ in order to obtain the desired decay (recall that our target is to obtained the truncation of an expansion that converges for all $|t| \leq 2$). We construct a sequence of functions, $(\mathbf{f}_m)$, as follows.

• ***Step 1.*** Let $\mathbf{f}_0 = (f_{1,0}, f_{2,0})$ where $f_{1,0} \equiv 0 \equiv f_{2,0}$, and consider the curve

$$\mathbf{C}_{\mathbf{f}_0}(t) = \mathbf{J}(\mathbf{f}_0)(t).$$

Choose a first integer $s_1 > 1$ and for each element of $\mathbf{N}(s_1)$, compute $\psi(\mathbf{f}_0)$ on this set of nodes and then deduce $\psi_{s_1}(\mathbf{f}_0)$ as described in the former subsection. Thanks to Proposition 2, Corollary 2.2 and Remark 2.2, the integer s_1 is chosen in such a way

$$\begin{aligned}&d(\psi_{s_1}(\mathbf{f}_0), \psi(\mathbf{f}_0)) \leq \nu \quad \text{and} \\ &d(\psi_{s_1}(\mathbf{f}_0), \psi_{s_1+k}(\mathbf{f}_0)) \leq \nu, \quad \forall\, k > 1.\end{aligned} \tag{40}$$

We set $\mathbf{f}_1 = \psi_{s_1}(\mathbf{f}_0)$.

• ***Step 2.*** Restart from Step 1, replacing $\mathbf{f}_0$ by $\mathbf{f}_1$, i.e. consider the curve

$$\mathbf{C}_{\mathbf{f}_1}(t) = \mathbf{J}(\mathbf{f}_1)(t).$$

Choose a second integer $s_2 \geq s_1$ and for each element of $\mathbf{N}(s_2)$, compute $\psi(\mathbf{f}_1)$ on this set of nodes and then deduce $\psi_{s_2}(\mathbf{f}_1)$. The integer s_2 is chosen in such a way

$$\begin{aligned}&d(\psi_{s_2}(\mathbf{f}_1), \psi(\mathbf{f}_1)) \leq \left(\frac{2}{3}\right)\nu \quad \text{and} \\ &d(\psi_{s_2}(\mathbf{f}_1), \psi_{s_2+k}(\mathbf{f}_1)) \leq \left(\frac{2}{3}\right)\nu, \quad \forall\, k > 1\end{aligned} \tag{41}$$

and such that

$$d(\psi_s(\mathbf{f}_1), \psi_s(\mathbf{f}_0)) \leq \frac{2}{3} d(\mathbf{f}_1, \mathbf{f}_0), \quad \forall\, s \geq s_2. \tag{42}$$

This latter condition is fulfilled thanks to Theorem 1. We set $\mathbf{f}_2 = \psi_{s_2}(\mathbf{f}_1)$. Observe that

$$\begin{aligned} d(\mathbf{f}_2, \mathbf{f}_1) &= d(\psi_{s_2}(\mathbf{f}_1), \psi_{s_1}(\mathbf{f}_0)) \\ &\leq d(\psi_{s_2}(\mathbf{f}_1), \psi_{s_2}(\mathbf{f}_0)) + d(\psi_{s_2}(\mathbf{f}_0), \psi_{s_1}(\mathbf{f}_0)), \end{aligned}$$

i.e. since $s_2 \geq s_1$, thanks to Eqs. (40) and (42)

$$d(\mathbf{f}_2, \mathbf{f}_1) \leq d(\psi_{s_2}(\mathbf{f}_1), \psi_{s_2}(\mathbf{f}_0)) + \nu$$

and therefore

$$d(\mathbf{f}_2, \mathbf{f}_1) \leq \frac{2}{3} d(\mathbf{f}_1, \mathbf{f}_0) + \nu.$$

Assuming, Step $2, \ldots, m-1$ to be reached.

• ***Step m.*** Restart from Step $m-1$, replacing $\mathbf{f}_{m-2}$ by $\mathbf{f}_{m-1}$, i.e. consider the curve

$$\mathbf{C}_{\mathbf{f}_{m-1}}(t) = \mathbf{J}(\mathbf{f}_{m-1})(t).$$

Choose a mth integer $s_m \geq s_{m-1}$ and for each element of $\mathbf{N}(s_m)$, compute $\psi(\mathbf{f}_{m-1})$ on this set of nodes and then deduce $\psi_{s_m}(\mathbf{f}_{m-1})$. The integer s_m is chosen in such a way

$$d(\psi_{s_m}(\mathbf{f}_{m-1}), \psi(\mathbf{f}_{m-1})) \leq \left(\frac{2}{3}\right)^{m-1} \nu$$

and

$$d(\psi_{s_m}(\mathbf{f}_{m-1}), \psi_{s_m+k}(\mathbf{f}_{m-1})) \leq \left(\frac{2}{3}\right)^{m-1} \nu, \quad \forall\, k > 1$$

and such that

$$d(\psi_s(\mathbf{f}_{m-1}), \psi_s(\mathbf{f}_{m-2})) \leq \frac{2}{3} d(\mathbf{f}_{m-1}, \mathbf{f}_{m-2}), \quad \forall\, s \geq s_m. \tag{43}$$

Observe that from the former steps, for $1 \leq j < m$, and for all $s \geq s_j$, we have

$$d(\psi_{s_j}(\mathbf{f}_{j-1}), \psi_{s_j+k}(\mathbf{f}_{j-1})) \leq \left(\frac{2}{3}\right)^{j-1} \nu, \quad \forall\, k > 1. \tag{44}$$

We set $\mathbf{f}_m = \psi_{s_m}(\mathbf{f}_{m-1})$. From Eqs. (43) and (44) we have

$$\begin{aligned} d(\mathbf{f}_m, \mathbf{f}_{m-1}) &= d(\psi_{s_m}(\mathbf{f}_{m-1}), \psi_{s_{m-1}}(\mathbf{f}_{m-2})) \\ &\leq d(\psi_{s_m}(\mathbf{f}_{m-1}), \psi_{s_m}(\mathbf{f}_{m-2})) \\ &\quad + d(\psi_{s_m}(\mathbf{f}_{m-2}), \psi_{s_{m-1}}(\mathbf{f}_{m-2})) \\ &\leq \frac{2}{3} d(\mathbf{f}_{m-1}, \mathbf{f}_{m-2}) + \left(\frac{2}{3}\right)^{m-2} \nu. \end{aligned}$$

We have constructed a sequence $(\mathbf{f}_m)$ that satisfies

$$d(\mathbf{f}_{m+2}, \mathbf{f}_{m+1}) \leq \frac{2}{3} d(\mathbf{f}_{m+1}, \mathbf{f}_m) + \left(\frac{2}{3}\right)^m \nu, \quad m \geq 0. \tag{45}$$

We apply Lemma 3, to the sequence $\mathbf{a}_m = d(\mathbf{f}_{m+1}, \mathbf{f}_m)$ and conclude that for all integer m, $n \geq 1$

$$\begin{aligned} d(\mathbf{f}_{m+n+1}, \mathbf{f}_m) &\leq \sum_{j=m}^{m+n} d(\mathbf{f}_{j+1}, \mathbf{f}_j) \\ &\leq 3 \left(\frac{2}{3}\right)^m d(\mathbf{f}_1, \mathbf{f}_0) + \nu \omega_m \end{aligned}$$

and therefore $(\mathbf{f}_m)$ is a Cauchy sequence. Therefore we choose $L \geq 1$, such that for all $k > 1$,

$$d(\mathbf{f}_{L-1}, \mathbf{f}_{L+k-1}) \leq \nu. \tag{46}$$

By construction we also have for all $k > 1$,

$$\begin{aligned} &\mathbf{d}(\psi_{s_L}(\mathbf{f}_{L-1}), \psi_{s_{L-1+k}}(\mathbf{f}_{L-1})) \leq \nu, \\ &d(\psi(\mathbf{f}_{L-1}), \psi_{s_{L+k-1}}(\mathbf{f}_{L-1})) \leq \nu. \end{aligned} \tag{47}$$

We set $\mathbf{f}_* = \mathbf{f}_{L-1}$. We have

$$\begin{aligned} \mathbf{d}(\mathbf{f}_*, \mathbf{h}_*) &\leq \mathbf{d}(\mathbf{f}_*, \psi_{s_L}(\mathbf{f}_*)) + \mathbf{d}(\psi_{s_L}(\mathbf{f}_*), \psi(\mathbf{f}_*)) \\ &\quad + \mathbf{d}(\psi(\mathbf{f}_*), \psi(\mathbf{h}_*)). \end{aligned} \tag{48}$$

Since $\mathbf{f}_* = \mathbf{f}_{L-1}$, we have that $\psi_{s_L}(\mathbf{f}_*) = \mathbf{f}_L$ and thanks to Eq. (46) we have

$$\mathbf{d}(\mathbf{f}_*, \psi_{s_L}(\mathbf{f}_*)) \leq \nu. \tag{49}$$

Furthermore, thanks to Proposition 1 we have

$$\mathbf{d}(\psi(\mathbf{f}_*), \psi(\mathbf{h}_*)) \leq \frac{1}{3} \mathbf{d}(\mathbf{f}_*, \mathbf{h}_*)$$

and from Eq. (48) we have

$$\begin{aligned} \frac{2}{3} \mathbf{d}(\mathbf{f}_*, \mathbf{h}_*) &\leq \mathbf{d}(\mathbf{f}_*, \mathbf{h}_*) - \mathbf{d}(\psi(\mathbf{f}_*), \psi(\mathbf{h}_*)) \\ &\leq \mathbf{d}(\mathbf{f}_*, \psi_{s_L}(\mathbf{f}_*)) + \mathbf{d}(\psi_{s_L}(\mathbf{f}_*), \psi(\mathbf{f}_*)). \end{aligned}$$

Thanks to Eqs. (47) and (49) we finally get

$$\mathbf{d}(\mathbf{f}_*, \mathbf{h}_*) \leq 3\nu,$$

which means that within the given tolerance ν, we can set $\mathbf{h}_* \sim \mathbf{f}_* = (f_{*1}, f_{*2})$.

We then deduce the parameterization of the local unstable manifold in the old coordinates by

writing

$$\begin{aligned}\mathbf{W}_{u,\mathrm{loc}}(t) &= \mathbf{T}(\mathbf{C}_{\mathbf{h}_*}(t))\\ &= \mathbf{p} + (\kappa t + t^2 h_{*,1}(t))\mathbf{U}_+\\ &\quad + t^2 h_{*,2}(t)\mathbf{U}_-,\end{aligned}$$

where $\mathbf{T}$ is defined in Eq. (8). We further extend this parameterization to get the global unstable manifold by writing

$$\mathbf{W}_u(t) = \bigcup_{n\geq 0} \Phi^n(\mathbf{W}_{u,\mathrm{loc}}(\mu^{-n}t)).$$

In the next section we illustrate our techniques for the case study Eq. (3) under consideration.

3. The van der Pol Hybrid Map

In order to parameterize the unstable manifold of a fixed point using the method described in Sec. 2, we need to locate a hyperbolic fixed (or periodic) point and compute the derivative of the hybrid map at this point to deduce the eigenvalues and associated eigenspaces. We also need to be able to compute the hybrid map and its derivative on a finite set of points. We accomplish these tasks by solving (numerically) the variational equation.

3.1. *The variational equation*

To achieve the forthcoming numerics, including the locus of the fixed point and later on the Taylor expansion of the local unstable manifold, we first need to estimate the time-τ map of the system Eq. (3) and its derivative with respect to initial conditions. As it is classical, we write the variational equation associated to Eq. (3) and integrate this latter using the Taylor integrator [Jorba & Zou, 2005; Lu *et al.*, 2016; Simo, 1990]. Once the variational equation is solved, we will be able to find the locus of a fixed point $\mathbf{p} = (p_1, p_2)$ thanks to Newton's method and deduce the eigenvalues of $d\Phi(\mathbf{p}) = d\mathbf{L} \circ d\mathcal{X}_\tau(\mathbf{p})$ as well as their corresponding eigenspaces.

Remark 3.1. Any integrator such as Runge–Kutta could be used instead of the Taylor integrator. The advantage with the latter comes from the fact that we can adjust the precision of each computation with two quantities: N, the number of terms in the expansion and K, the number of steps, see below for more details.

Let $(x(t), y(t))$ be the solution of Eq. (3) with initial condition (x_0, y_0). We write

$$\frac{\partial x}{\partial x_0} = \xi_1, \quad \frac{\partial x}{\partial y_0} = \xi_2, \quad \frac{\partial y}{\partial x_0} = \zeta_1, \quad \frac{\partial y}{\partial y_0} = \zeta_2.$$

From Eq. (3) and after differentiation, the variational equation is given by

$$\hat{\mathcal{X}} : \begin{cases} \dot{x} = y - \alpha\left(\dfrac{x^3}{3} - x\right),\\ \dot{y} = -x,\\ \dot{\xi}_1 = \zeta_1 - \alpha(x^2-1)\xi_1,\\ \dot{\xi}_2 = \zeta_2 - \alpha(x^2-1)\xi_2,\\ \dot{\zeta}_1 = -\xi_1,\\ \dot{\zeta}_2 = -\xi_2. \end{cases} \tag{50}$$

We denote by $\hat{\mathcal{X}}_t(P)$ the solution of Eq. (50) with initial condition

$$P = (x, y, \xi_1, \xi_2, \zeta_1, \zeta_2)$$

and our final goal is to compute

$$\hat{\mathcal{X}}_\tau(P_0), \quad \text{with } P_0 = (x_0, y_0, 1, 0, 0, 1),$$

$$d\Phi(x,y) = d\mathbf{L} \circ d\mathcal{X}_\tau(x,y) = \begin{pmatrix} \xi_1(\tau) & \xi_2(\tau) \\ \zeta_1(\tau) & \zeta_2(\tau) \end{pmatrix}. \tag{51}$$

Let $N > 1$ be a large integer. The Taylor expansion of Eq. (50) at the time t with initial condition P can be written as

$$\hat{\mathcal{X}}_t(P) = \hat{\mathcal{X}}_{t,N}(P) + \mathcal{R}_{t,N}(P),$$

where

$$\hat{\mathcal{X}}_{t,N}(P) = \sum_{j=0}^{N} t^j \mathbf{A}_j(P)$$

and where $\mathcal{R}_{t,N}(P)$ represents the reminder. The $\mathbf{A}_j$'s are vectors and are computed in such a way that $\hat{\mathcal{X}}_0(P) = P$, i.e. $\mathbf{A}_0(P) = P$ and

$$\frac{\partial}{\partial t}\hat{\mathcal{X}}_t(P) = \hat{\mathcal{X}}\left(\sum_{j=0}^{N} t^j \mathbf{A}_j(P) + \sum_{j=N}^{\infty} t^j \mathbf{A}_j(P)\right). \tag{52}$$

Thanks to Eq. (50), collecting term of order k in t on the left-hand side of Eq. (52) and identifying these

with the terms of order k in t on the right-hand side leads to

$$\mathbf{A}_1(P) = \hat{\mathcal{X}}(P) = \left(y - \alpha\left(\frac{x^3}{3} - x\right), -x, \zeta_1 - \alpha(x^2-1)\xi_1, \zeta_2 - \alpha(x^2-1)\xi_2, -\xi_1, -\xi_2\right)$$

and for all $k \geq 1$,

$$\begin{aligned}\mathbf{A}_{k+1} &= (A_{k+1,1}, A_{k+1,2}, A_{k+1,3}, A_{k+1,4}, A_{k+1,5}, A_{k+1,6}) \\ &= \begin{pmatrix} \dfrac{1}{k+1}\left(A_{k,2} + \alpha\left(A_{k,1} - \left(\dfrac{1}{3}\right)\displaystyle\sum_{j=0}^{k}\sum_{i=0}^{j} A_{k-j,1}A_{i,1}A_{j-i,1}\right)\right) \\ -\dfrac{A_{k,1}}{k+1} \\ \dfrac{1}{k+1}\left(A_{k,5} + \alpha\left(A_{k,3} - \displaystyle\sum_{j=0}^{k}\sum_{i=0}^{j} A_{k-j,3}A_{i,1}A_{j-i,1}\right)\right) \\ \dfrac{1}{k+1}\left(A_{k,6} + \alpha\left(A_{k,4} - \displaystyle\sum_{j=0}^{k}\sum_{i=0}^{j} A_{k-j,4}A_{i,1}A_{j-i,1}\right)\right) \\ -\dfrac{A_{k,3}}{k+1} \\ -\dfrac{A_{k,4}}{k+1} \end{pmatrix}. \end{aligned} \tag{53}$$

We expect the remainder to be of the same order as the "first missing term", that is

$$\|\mathcal{R}_{t,N}(x,y)\| = \mathcal{O}(\|\mathbf{A}_{N+1}\||t|^{N+1}).$$

We will be more specific about the choice of N shortly. For values of τ sufficiently small, $\hat{\mathcal{X}}_{\tau,N}$ is a good approximation of $\hat{\mathcal{X}}_\tau$. However, when τ becomes large, this approximation is no longer accurate. To solve this problem, we subdivide the time interval $[0,\tau]$, choosing mesh points

$$0 = \tau_0 < \tau_1 < \cdots < \tau_{K-1} < \tau_K = \tau, \quad \text{so that}$$
$$\tau_{j+1} - \tau_j = \frac{\tau}{K}, \ \ j = 1, \ldots, K-1.$$

Observe that the mesh points chosen do not need to be equally distributed, for instance, it is typical to instead use Chebyshev nodes, see [Lessard *et al.*, 2015; Lu *et al.*, 2016; James & Mischaikow, 2014] for more examples and discussions.

We then replace $\hat{\mathcal{X}}_{\tau,N}$ with the composition

$$\hat{\mathcal{X}}_{\tau,N,K} = \hat{\mathcal{X}}_{\tau/K,N} \circ \hat{\mathcal{X}}_{\tau/K,N} \circ \cdots \circ \hat{\mathcal{X}}_{\tau/K,N} \circ \hat{\mathcal{X}}_{\tau/K,N}.$$

The map Φ is then approximated by

$$\mathbf{\Phi}(x,y) \simeq \mathbf{L} \circ \mathcal{X}_{\tau,N,K}(x,y), \tag{54}$$

where $\mathcal{X}_{\tau,N,K}(x,y)$ represents the first two components of $\hat{\mathcal{X}}_{\tau,N,K}(P)$. Since $\mathcal{X}$ is analytic, it follows that for any $\epsilon > 0$, there exists K_ϵ, N_ϵ such that

$$\|\Phi - \mathbf{L} \circ \hat{\mathcal{X}}_{\tau,N_\epsilon,K_\epsilon}\|_\infty < \epsilon.$$

In this work, we do not make any attempt to validate this error bound for any choice of K, N or ϵ although numerical techniques for this do exist. However, for all computations in this paper we have chosen K, N such that the last coefficient in the Taylor expansion of $\hat{\mathcal{X}}_{\tau/K,N}$ for each factor in the composition defining $\hat{\mathcal{X}}_{\tau,N,K}$ has norm on the order 10^{-20}.

Thanks to the variational equation and the Newton method, we are now able to compute the locus of a fixed point of saddle type. For $\alpha = 2$, $\beta = 2.7$ and $\tau = 3.4$, our computation reveals

$$\mathbf{p} \simeq (0.048582402779739, 0.1900388885500928)$$

and the eigenvalues of $d\Phi(\mathbf{p})$ are

$$\mu \simeq -8.98587910633646 \quad \text{and}$$

$$\lambda \simeq -0.411572739299455.$$

For associated eigenvectors, both $\mathbf{U}_+$ and $\mathbf{U}_-$ are expressed in Eq. (4) with

$$\mathrm{U}_{+,1} = 1, \quad \mathrm{U}_{+,2} \simeq 0.02988522473991$$

and

$$\mathrm{U}_{-,1} \simeq -0.3446813141376327, \quad \mathrm{U}_{-,2} = 1.$$

3.2. *Numerics for the local unstable manifold*

Using the estimate given in Eq. (54), the change of coordinates defined in Eq. (9) and following the steps described in Sec. 2, we compute a parameterization of the local unstable manifold. More precisely we choose $\nu = 10^{-16}$, and we approximate $\mathbf{\Phi}$ by choosing $K = 35$ and $N = 30$. Both choices were made based on a numerical verification that this yields a Taylor expansion satisfying the scheme described in the previous section.

Furthermore by choosing $\kappa = 1/5$, and the same number of node $s = 22$ for each step (described in Sec. 2.6), we observe a convergence of the sequence $(\mathbf{f}_m)$ after $m = 18$ iterates of ψ_s, i.e. for all $k \geq 0$

$$\mathbf{d}(\mathbf{f}_{18}, \mathbf{f}_{k+18}) \leq \nu,$$

where in the present case

$$\mathbf{f}_{k+18} = \psi_{22}(\mathbf{f}_{k-1+18}).$$

Thus, we have

$$\mathbf{W}_{u,\mathrm{loc}}(t) \sim \mathbf{T} \circ \mathbf{f}_{18}(t) = \sum_{j=0}^{23} t^j \mathbf{B}_j, \tag{55}$$

where the $\mathbf{B}_j's$ are the vector valued coefficients of the above polynomial expansion. The first ten coefficients are displayed in Table 1. We stopped the iteration after 18 steps because all of the digits reported in Table 1 were fixed upon further iteration which is a heuristic indication (though certainly not a proof) that the iteration has converged.

3.3. A posteriori *analysis*

In this subsection we describe numerical, *a posteriori* analysis of our numerical approximation for the unstable manifold. These estimates are heuristic in nature, however, they provide a compelling evidence which suggests that our computations are highly accurate.

Table 1.

$\mathbf{B}_0 = (0.048582402779739, 0.190038888550092)$
$\mathbf{B}_1 = (0.2, 0.005977044947983)$
$\mathbf{B}_2 = (-0.002192096233904, 0.008329139135282)$
$\mathbf{B}_3 = (-0.000436494302159, 0.000735901354063)$
$\mathbf{B}_4 = (0.0000686845574053, 0.0000569934110486)$
$\mathbf{B}_5 = (2.3690010373 * 10^{-6}, 6.3196972321 * 10^{-6})$
$\mathbf{B}_6 = (-4.37600643 * 10^{-7}, 6.64638568 * 10^{-7})$
$\mathbf{B}_7 = (1.8413431 * 10^{-8}, 6.12767048 * 10^{-8})$
$\mathbf{B}_8 = (3.594325 * 10^{-9}, 6.1650781 * 10^{-9})$
$\mathbf{B}_9 = (-2.861118 * 10^{-10}, 6.49829 * 10^{-10})$

We begin by remarking that Table 1 strongly suggests that for $\kappa = 1/5$ our numerical approximation of the unstable manifold converges for all $|t| \leq 2$. Recall that

$$\mathbf{W}_{u,\mathrm{loc}}(t) = \sum_{j=0}^{\infty} t^j \mathbf{w}_j \tag{56}$$

the (exact) expansion of the unstable manifold with

$$\mathbf{w}_0 = \mathbf{p}, \quad \mathbf{w}_1 = \kappa \mathbf{U}_+.$$

Within the chosen precision (i.e. $\nu = 10^{-16}$) we claim that the $\mathbf{B}_j$'s coincide with the $\mathbf{w}_j's$, more precisely

$$\|\mathbf{B}_j - \mathbf{w}_j\| \leq \mathcal{O}(\nu).$$

To verify the above we perform the following tests.

(i) We recompute the coefficients $\mathbf{B}_j$'s with more nodes, $s = 24, 26, \ldots$ and at each time, we observe that the coefficients of the new expansion coincides (within the ν precision) with the former.

(ii) Since the expansion given in Eq. (56) converges for all $|t| \leq 2$, we must have

$$\mathbf{\Phi}(\mathbf{W}_{u,\mathrm{loc}}(t)) = \mathbf{W}_{u,\mathrm{loc}}(\mu t), \quad \forall\, |t| \leq 2.$$

We first verify, (within the ν precision) that this latter property also holds for Eq. (55) for all $|t| \leq 1$, i.e.

$$\|\mathbf{\Phi}(\mathbf{T} \circ \mathbf{f}_{18}(t)) - \mathbf{T} \circ \mathbf{f}_{18}(t)(\mu t)\| \leq \mathcal{O}(\nu), \quad \forall\, |t| \leq 1.$$

The expansion in (56) can be approximated with a polynomial of degree 23 using $\mathbf{T} \circ \mathbf{f}_{18}$, i.e. Eq. (55),

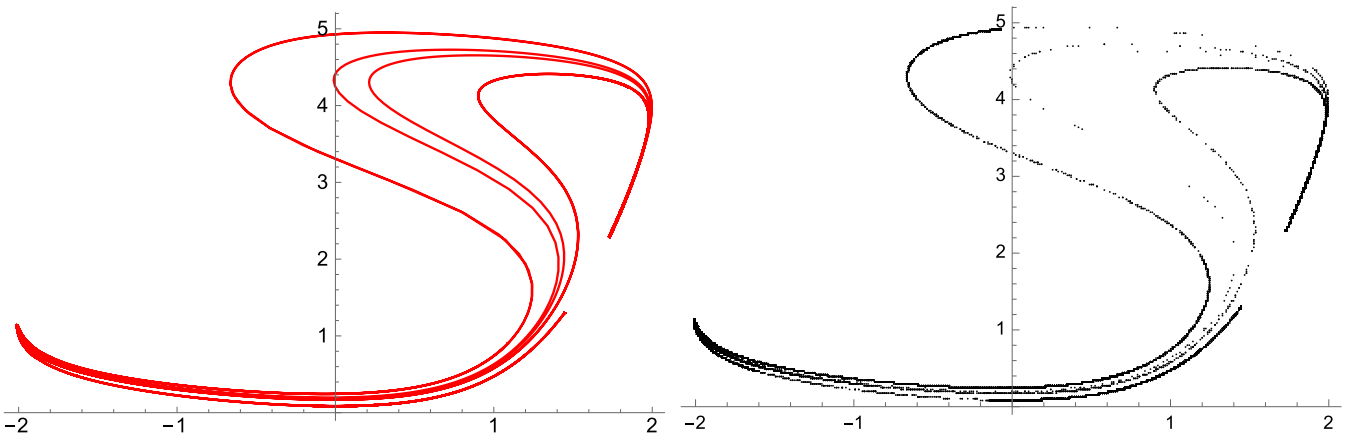

Fig. 1. (Left) The unstable manifold of the fixed point $\mathbf{p}$. (Right) The attractor of the system.

but also by truncating Eq. (56) at the order 23, i.e.

$$\mathbf{W}_{u,\mathrm{loc}}(t) \sim \mathbf{W}_{u,23}(t) = \sum_{j=0}^{23} t^j \mathbf{w}_j.$$

The above polynomial satisfies

$$\|\boldsymbol{\phi}(\mathbf{W}_{u,23}(t)) - \mathbf{W}_{u,23}(\mu t)\| \leq \mathcal{O}(\|\mathbf{w}_{24}\||t|^{23}), \quad \forall\, |t| \leq 2.$$

We then verify that the above estimate also holds for the expansion given in Eq. (55) i.e.

$$\|\boldsymbol{\phi}(\mathbf{T} \circ \mathbf{f}_{18}(t)) - \mathbf{T} \circ \mathbf{f}_{18}(\mu t)\| \leq \mathcal{O}(\|\mathbf{B}_{24}\||t|^{24}), \quad \forall\, |t| \leq 2,$$

where $\mathbf{B}_{24}$ was estimated in (i).

3.4. *A strange attractor near a homoclinic orbit*

Figure 1, on the top, displays part of the global unstable manifold (in red). More precisely, we plot

$$\{\mathbf{W}_u(t) \sim \Phi^7(\mathbf{T} \circ \mathbf{f}_{18}(\mu^{-7}t)), |t| \leq 20.\}.$$

By plotting the orbit of a point $\mathbf{q}$ randomly chosen in the rectangle $\mathbf{K} = [-2, 2] \times [0, 5]$ and ignoring the first iterates, i.e.

$$\{\boldsymbol{\Phi}^n(\mathbf{q}), 100\,000 \leq n \leq 600\,000\}$$

we emphasize the presence of an attractor displayed at the bottom of Fig. 1. On the top of Fig. 2, we superimpose the plot of the unstable manifold displayed on the top of Fig. 1 (in red), with the local stable manifold (in blue), emphasizing (at least) two transverse homoclinic intersections. The local stable manifold is computed using the same method for the

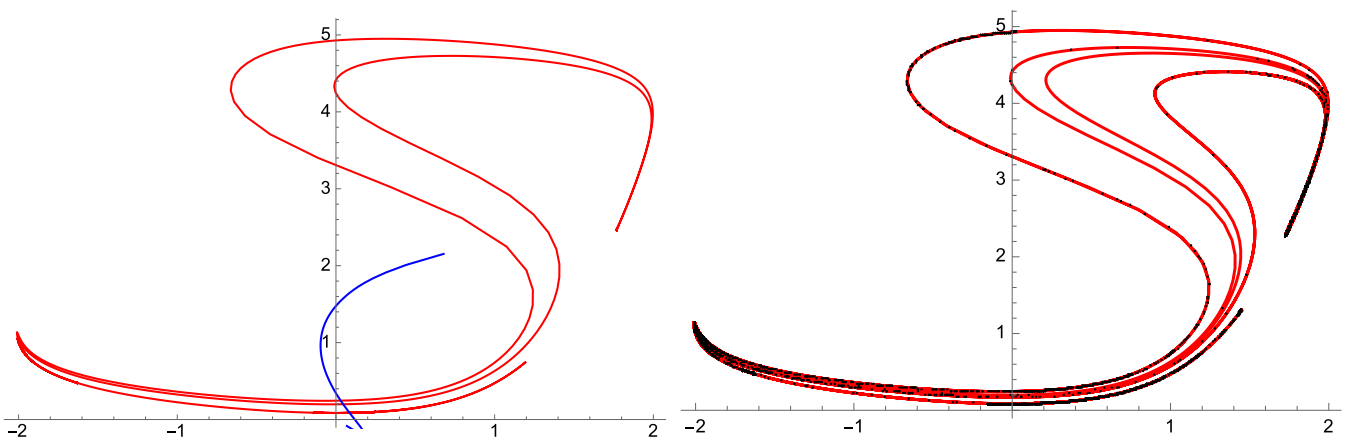

Fig. 2. (Left) Part of the unstable manifold (red) with the stable manifold (blue). (Right) The unstable manifold (red) superimposed with the attractor (black).

unstable manifold replacing $\mathbf{\Phi}$ by $\mathbf{\Phi}^{-1} = \mathcal{X}_{-\tau} \circ \mathbf{L}^{-1}$. These homoclinic intersections guarantee the system to be chaotic. At the bottom of Fig. 2, the attractor is superimposed with the global unstable manifold, suggesting that the former is included in the closure of the unstable manifold.

3.5. *A positive Lyapunov exponent*

With the same point $\mathbf{q} \in \mathbf{K}$ chosen to plot the orbit displayed at the bottom of Fig. 1 and mimicking the attractor, we choose

$$\mathbf{z} = \Phi^L(\mathbf{q}), \quad L \sim 200\,000$$

this point being close to the attractor. We choose

$$\mathbf{v} = \begin{pmatrix} 1 \\ 1 \end{pmatrix}$$

and for each integer n, we compute

$$\ell_n = \frac{1}{n} \log \|D\mathbf{\Phi}^n(\mathbf{z})(\mathbf{v})\|$$

and our numerics reveals that for $30\,000 \leq n \leq 100\,000$,

$$\ell_n \sim 0.3009.$$

This value is retrieved when changing the vector $\mathbf{v}$ by any other vector, suggesting this attractor to possess a positive Lyapunov exponent. Since this attractor is already transitive by construction, we infer that the invariant set displayed at the bottom of Fig. 1 is a strange attractor, see for instance [Mora & Viana, 1993] for more details.

3.6. *Further discussion*

The similarity between the two pictures in Fig. 1 leads us to make the following conjecture. The closure of the unstable manifold of $\mathbf{p}$ contains the global attractor for $\mathbf{\Phi}$. While answering this question is beyond the scope of the present work, we remark that similar results have been proved using rigorous numerical and topological methods. An approach for investigating this conjecture would be to compute a rigorous outer approximation of the unstable manifold for $\mathbf{p}$. From an outer approximation, topological and combinatorial methods exist for extracting the dynamics (see [Fontaine *et al.*, 2016; Kalies *et al.*, 2017; Miyaji *et al.*, 2016]) or computing topological entropy (see [Day *et al.*, 2008; Day & Frongillo, 2019]), and software based on these methods is available (e.g. [Kalies, 2016]). Typically, these approaches obtain the required outer approximation for an explicitly defined map by computing with an interval arithmetic library e.g. [Rump, 1999]. However, when considering the map $L \circ \mathcal{X}_\tau$ in which case there is no explicit formula for $\mathcal{X}_\tau$, the approach become more challenging and obtaining an outer approximation is not so straightforward. Nevertheless, there are rigorous numerical methods for enclosing solutions of $\mathcal{X}_\tau$, see for example [Berz & Makino, 1998; Arioli & Koch, 2015; Zgliczynski, 2002]. These methods also extend to enclosing surfaces of initial conditions [Kalies *et al.*, 2018]. Approaches based on computing outer approximations for the time-τ map of a flow have already been combined with topological methods to compute combinatorial dynamics and obtain rigorous proofs of complicated dynamics such as chaos or existence of strange attractors (see e.g. [Kepley & James, 2019; Mischaikow & Mrozek, 1995; Tucker, 1999, 2002; Wilczak, 2003]).

References

Arioli, G. & Koch, H. [2015] "Existence and stability of traveling pulse solutions of the Fitzhugh–Nagumo equation," *Nonlin. Anal.* **113**, 51–70.

Benedicks, M. & Carlson, L. [1991] "The dynamics of the Hénon map," *Ann. Math.* **133**, 73–169.

Berz, M. & Makino, K. [1998] "Verified integration of odes and flows using differential algebraic methods on high-order Taylor models," *Reliab. Comput.* **4**, 361–369.

Cabré, X., Fontich, E. & de la Llave, R. [2003] "The parameterization method for invariant manifolds. I. Manifolds associated to non-resonant subspaces," *Indiana Univ. Math. J.* **52**, 283–328.

Cabré, X., Fontich, E. & de la Llave, R. [2005] "The parameterization method for invariant manifolds. III. Overview and applications," *J. Diff. Eqs.* **218**, 444–515.

Day, S., Frongillo, R. & Treviño, R. [2008] "Algorithms for rigorous entropy bounds and symbolic dynamics," *SIAM J. Appl. Dyn. Syst.* **7**, 1477–1506.

Day, S. & Frongillo, R. [2019] "Sofic shifts via conley index theory: Computing lower bounds on recurrent dynamics for maps," *SIAM J. Appl. Dyn. Syst.* **18**, 1610–1642.

Fontaine, M., Kalies, W. D. & Naudot, V. [2016] "Chaos near a resonant inclination-flip," *Physica D* **334**, 141–157.

Franceschini, V. & Russo, L. [1981] "Stable and unstable manifolds of the Hénon mapping," *J. Statist. Phys.* **25**, 757–769.

Gonzalez, J. & James, J. M. [2017] "High-order parameterization of stable/unstable manifolds for long periodic orbits of maps," *SIAM J. Appl. Dyn. Syst.* **16**, 1748–1795.

Guckenheimer, J. & Holmes, P. [1983] *Nonlinear Oscillations, Dynamical Systems, and Bifurcations of Vector Fields* (Applied Mathematical Sciences).

Handscomb, D. & Mason, J. [2002] *Chebyshev Polynomials* (CRC Press).

Haro, À. & de la Llave, R. [2006] "A parameterization method for the computation of invariant tori and their whiskers in quasi-periodic maps: Numerical algorithms," *Discr. Contin. Dyn. Syst. Ser. B* **6**, 1261–1300.

Heagy, J. F. [1992] "A physical interpretation of the Hénon map," *Physica D* **57**, 436–446.

Hénon, M. [1976] "A two-dimensional mapping with a strange attractor," *Comm. Math. Phys.* **50**, 69–77.

Hirsch, M., Pugh, C. & Shub, M. [1977] *Invariant Manifolds*, Vol. 583 (Lect. Notes Math. Springer).

Ippolito, S. & Naudot, V. [2016] "Implicit fox rabies model with an asymptotic computation of chaos," *Electron. J. Biol.* **12**, 402–409.

Ippolito, S., Naudot, V. & Noonburg, E. [2016] "Alternative stable states, coral reefs, and smooth dynamics with a kick," *Bull. Math. Biol.* **78**, 413–135.

James, J. D. M. & Mischaikow, K. [2014] "Computational proofs in dynamics," to appear.

James, J. D. M. [2020] "Fourier–Taylor approximation of unstable manifolds for compact maps: Numerical implementation and computer assisted error bounds," submitted.

Jorba, À. & Zou, M. [2005] "A software package for the numerical integration of ODEs by means of high-order Taylor methods," *Experim. Math.* **14**, 99–117.

Kalies, W. [2016] "Computational dynamics software (CDS) ver. 2.1," http://math.fau.edu/kalies/CDS.

Kalies, W. D., Kasti, D. & Vandervorst, R. [2017] "An algorithmic approach to lattices and order in dynamics," *SIAM J. Appl. Dyn. Syst.* **17**, 1617–1649.

Kalies, W., Kepley, S. & James, J. M. [2018] "Analytic continuation of local (un)stable manifolds with rigorous computer assisted error bounds," *SIAM J. Appl. Dyn. Syst.* **17**, 157–202.

Kepley, S. & James, J. M. [2019] "Chaotic motions in the restricted four body problem via devaney's saddle-focus homoclinic tangle theorem," *J. Diff. Eqs.* **266**, 1709–1755.

Krauskopf, B., Osinga, H. M., Doedel, E. J., Henderson, M., Guckenheimer, J., Vladimirsky, A., Dellnitz, M. & Junge, O. [2005] "A survey of methods for computing (un)stable manifolds of vector fields," *Int. J. Bifurcation and Chaos* **15**, 763–791.

Lessard, J. P., van den Berg, J. B., James, J. D. M. & Mischaikow, K. [2011] "Rigorous numerics for symmetric connecting orbits: Even homoclinics of the Gray–Scott equation," *SIAM J. Math. Anal.* **43**, 1557–1594.

Lessard, J. P., James, J. D. M. & Reinhardt, C. [2014] "Computer assisted proof of transverse saddle-to-saddle connecting orbits for first order vector fields," *J. Dyn. Diff. Eqs.* **26**, 267–313.

Lessard, J., Castelli, R. & Jamese, J. D. [2015] "Parameterization of invariant manifolds for periodic orbits I: Efficient numerics via the Floquet normal form fields," *SIAM J. Appl. Dyn. Syst.* **14**, 132–167.

Lin, K. & Young, L. [2010] "Dynamics of periodically-kicked oscillators," *J. Fixed Point Th. Appl.* **7**, 291–312.

Lu, Q., Mireles-James, J. & Naudot, V. [2016] "High-order parameterization of (un)stable manifolds for hybrid maps: Implementation and applications," *Commun. Nonlin. Sci. Numer. Simul.* **53**, 184–201.

Martens, M., Naudot, V. & Yang, J. [2006] "A strange attractor with large entropy in the unfolding of a low resonant degenerate homoclinic orbit," *Int. J. Bifurcation and Chaos* **16**, 3509–3522.

Mischaikow, K. & Mrozek, M. [1995] "Chaos in the Lorenz equations: A computer-assisted proof," *Bull. Amer. Math. Soc.* (*N.S.*) **32**, 66–72.

Miyaji, T., Pilarczyk, P., Gameiro, M., Kokubu, H. & Mischaikow, K. [2016] "A study of rigorous ode integrators for multi-scale set-oriented computations," *Appl. Numer. Math.* **107**, 34–47.

Mora, L. & Viana, M. [1993] "Abundance of strange attractors," *Acta Math* **171**, 1–71.

Naudot, V. [1996] "Strange attractors in the unfolding of an inclination-flip homoclinic orbit," *Ergod. Th. Dyn. Syst.* **16**, 1071–1086.

Naudot, V. [2002] "A strange attractor in the unfolding of an orbit-flip homoclinic orbit," *Dyn. Syst.* **17**, 45–63.

Palis, J. & de Melo, W. [1980] *Geometric Theory of Dynamical Systems: An Introduction* (Springer-Verlag).

Palis, J. & Takens, F. [1993] *Hyperbolicity and Sensitive Chaotic Dynamics at Homoclinic Bifurcations*, Vol. 35 (Cambridge University Press).

Rump, S. [1999] *Developments in Reliable Computing* (Kluwer Academic Publishers), pp. 77–104.

Ryals, B. & Young, L. S. [2012] "Horseshoes of periodically-kicked van der Pol oscillators," *Chaos* **22**, 043140.

Rychlik, M. [1990] "Lorenz attractors through Shil'nikov-type bifurcation. Part 1," *Ergod. Th. Dyn. Syst.* **10**, 793–821.

Simo, C. [1990] *On the Analytical and Numerical Approximation of Invariant in Modern Methods in Celestial Mechanics, Comptes Rendus de la 13ieme Ecole Printemps d'Astrophysique de Goutelas*

Manifolds (Daniel Benest and Claude Froeschle. Gif-sur-Yvette), p. 285.

Tucker, W. [1999] "The Lorenz attractor exists," *C. R. Acad. Sci. Paris Sér. I Math.* **328**, 1197–1202.

Tucker, W. [2002] "A rigorous ode solver and Smale's 14th problem," *Found. Comput. Math.* **2**, 53–117.

van den Berg, J. B., Mireles-James, J. D., Lessard, J. P. & Mischaikow, K. [2011] "Rigorous numerics for symmetric connecting orbits: Even homoclinics of the Gray–Scott equation," *SIAM J. Math. Anal.* **4**, 1557–1594.

van der Pol, B. & van der Mark, J. [1927] "Frequency demultiplication," *Nature* **120**, 363–364.

Wang, Q. & Young, L. S. [2008] "Toward a theory of rank one attractors," *Ann. Math.* **167**, 349–480.

Wilczak, D. [2003] "Chaos in the Kuramoto–Sivashinsky equations — A computer-assisted proof," *J. Diff. Eqs.* **194**, 433–459.

Zgliczynski, P. [2002] "c^1 Lohner algorithm," *Found. Comput. Math.* **2**, 429–465.